CORA Cork Open Research Archive
Cartlann Taighde Oscailte Chorcaí

| | |
|---|---|
| Title | DNA sensor associated type I Interferon signalling is increased in ulcerative colitis and induces JAK-dependent inflammatory cell death in colonic organoids |
| Authors | Flood, Peter;Fanning, Aine;Woznicki, Jerzy A.;Crowley, Tadhg;Christopher, Andrea;Vaccaro, Alessandra;Houston, Aileen M.;McSweeney, Sheila;Ross, Sarah;Hogan, Aileen;Brint, Aileen;Skowyra, Agnieszka;Bustamante, Milan;Ambrose, Monica;Moloney, Gerard M.;MacSharry, John;Hammarström, Marie-Louise;Hurley, Margot;Fitzgibbons, Christine;Quigley, Eamonn M. M.;Shanahan, Fergus;Zulquernain, Syed A.;McCarthy, Jane;Dodson, G. Steven;Dabbagh, Karim;McRae, Bradford L.;Melgar, Silvia;Nally, Ken |
| Publication date | 2022-09-27 |
| Original Citation | Flood, P., Fanning, A., Woznicki, J. A., Crowley, T., Christopher, A., Vaccaro, A., Houston, A., McSweeney, S., Ross, S., Hogan, A., Brint, A., Skowyra, A., Bustamante, M., Ambrose, M., Moloney, G. M., MacSharry, J., Hammarström, M.-L., Hurley, M., Fitzgibbons, C., Quigley, E. M. M., Shanahan, F., Zulquernain, S. A., McCarthy, J., Dodson, G. S., Dabbagh, K., McRae, B. L., Melgar, S. and Nally, K. (2022) 'DNA sensor associated type I Interferon signalling is increased in ulcerative colitis and induces JAK-dependent inflammatory cell death in colonic organoids', American Journal of Physiology - Gastrointestinal and Liver Physiology, 323(5), pp 439-460. https://doi.org/10.1152/ajpgi.00104.2022 |
| Type of publication | Article (peer-reviewed) |
| Link to publisher's version | 10.1152/ajpgi.00104.2022 |
| Rights | © 2022, American Physiological Society. All rights reserved. This is a post-peer-review, pre-copyedit version of an article published in American Journal of Physiology - Gastrointestinal and Liver Physiology. The final authenticated version is available online at: https://doi.org/10.1152/ajpgi.00104.2022 |
| Download date | 2026-11-16 14:15:03 |

| | |
|---|---|
| Item downloaded from | https://hdl.handle.net/10468/13724 |



# DNA sensor associated type I Interferon signalling is increased in ulcerative colitis and induces JAK-dependent inflammatory cell death in colonic organoids

Peter Flood[1,*], Aine Fanning[1,*], Jerzy A. Woznicki[1], Tadhg Crowley[1], Andrea Christopher[1], Alessandra Vaccaro[1], Aileen Houston[1,2], Sheila McSweeney[1], Sarah Ross[1], Aileen Hogan [1], Elizabeth Brint[1,3], Agnieszka Skowyra[1], Milan Bustamante[1], Monica Ambrose[1], Gerard Moloney[1], John MacSharry[1,4], Marie-Louise Hammarström[5], Margot Hurley[1,2], Christine Fitzgibbons[1], Eamonn MM Quigley[1], Fergus Shanahan[1,2], Syed A. Zulquernain[1,2], Jane McCarthy[6], G. Steven Dodson[7], Karim Dabbagh[7], Bradford L. McRae[8], Silvia Melgar[1], Ken Nally[†,1,9]

[1]APC Microbiome Ireland, University College Cork, Cork, Ireland
[2]Department of Medicine, University College Cork, Cork, Ireland
[3]Department of Pathology, Cork University Hospital, University College Cork, Clinical Sciences Building, Cork, Ireland
[4]Schools of Microbiology and Medicine, University College Cork, Ireland
[5]Department of Clinical Microbiology, Section of Infection and Immunology, Umeå University, Umeå, Sweden
[6]Department of Gastroenterology, Mercy University Hospital, Cork, Ireland
[7]Second Genome, Brisbane, CA, USA
[8]Immunology Discovery, Abbvie Bioresearch Center, Worcester, MA 01605, USA
[9]School of Biochemistry and Cell Biology, University College Cork, Cork, Ireland

**Short Title: IFN-β & TNF-α induce inflammatory cell death in organoids**

* These authors contributed equally to this work

†Corresponding author

**Ken Nally, Ph.D.**
Host-Microbe and Gut Inflammation Group
APC Microbiome Ireland
School of Biochemistry and Cell Biology
Rm. 2.10, Biosciences Building
University College Cork
College Road, Cork, Ireland
T: 00353-21-4901302
E: k.nally@ucc.ie



Downloaded from journals.physiology.org/journal/ajpgi at Univ Col Cork (143.239.045.011) on October 3, 2022.

**Abstract**

DNA sensor pathways can initiate inflammasome, cell death and type I interferon (IFN) signalling in immune-mediated inflammatory diseases (IMIDs); including type I interferonopathies. We investigated the involvement of these pathways in the pathogenesis of ulcerative colitis (UC); by analysing expression of DNA sensor, inflammasome, and type I IFN biomarker genes in colonic mucosal biopsy tissue from control (n=31), inactive UC (n=31), active UC (n=33) and a UC single cell RNA-Seq dataset. The effects of type I IFN (IFN-β), IFN-γ and TNF-α on gene expression, cytokine production and cell death were investigated in human colonic organoids. In organoids treated with cytokines alone, or in combination with NLRP3, caspase or JAK inhibitors, cell death was measured, and supernatants were assayed for IL-1β/IL-18/CXCL10. The expression of DNA sensor pathway genes - PYHIN family members (*AIM2*, *IFI16*, *MNDA*, *PYHIN1*), as well as *ZBP1*, *cGAS* and *DDX41* were increased in active UC and expressed in a cell type restricted pattern. Inflammasome genes (*CASP1*, *IL1B*, *IL18*), type I IFN inducers (*STING*, *TBK1*, *IRF3*), *IFNB1* and type I IFN biomarker genes (*OAS2*, *IFIT2*, *MX2*) were also increased in active UC. Co-treatment of organoids with IFN-β or IFN-γ and TNFα increased expression of *IFI16*, *ZBP1*, *CASP1*, *cGAS* and *STING*, induced cell death and IL-1β/IL-18 secretion. This inflammatory cell death was blocked by the JAK inhibitor tofacitinib but not by inflammasome or caspase inhibitors. Increased type I IFN activity may drive elevated expression of DNA sensor genes and JAK-dependent but inflammasome-independent inflammatory cell death of colonic epithelial cells in UC.

**Keywords: Ulcerative colitis, epithelium, interferon, inflammasome, JAK inhibitor**



Downloaded from journals.physiology.org/journal/ajpgi at Univ Col Cork (143.239.045.011) on October 3, 2022.

**NEW & NOTEWORTHY** This study found that patients with active UC have significantly increased colonic gene expression of cytosolic DNA sensor, inflammasome, STING and type I IFN signalling pathways. The type I IFN - IFN-β - in combination with TNF-α induced JAK-dependent but NLRP3 and inflammasome-independent inflammatory cell death of colonic organoids. This novel inflammatory cell death phenotype is relevant to UC immunopathology; and may partially explain the efficacy of the JAKinibs tofacitinib and upadacitinib in patients with UC.

**Supplemental material available at:**

DOI: https://doi.org/10.6084/m9.figshare.19626630

URL: https://figshare.com/s/97da7a00f3d857e9ee34



Downloaded from journals.physiology.org/journal/ajpgi at Univ Col Cork (143.239.045.011) on October 3, 2022.

## 1 Introduction

Crohn's disease (CD) and ulcerative colitis (UC) are the most common forms of inflammatory bowel disease (IBD), characterised by chronic and relapsing intestinal inflammation. The interaction of multiple genetic, environmental and immune factors drive disease, but the exact aetiology and pathogenesis of IBD is not fully understood (1, 2). Dysfunctional host-microbe interactions underpinned by pattern recognition receptor (PRR) signalling are known to promote intestinal inflammation and are strongly linked to IBD (3, 4).

Cytosolic DNA sensors are an important family of PRRs (5), implicated in many immune-mediated inflammatory diseases (IMIDs) including type I interferonopathies but are generally less well characterised in the context of IBD (6). They can detect DNA from self (mitochondrial DNA (mtDNA), nuclear fragments) and non-self (commensal microbes and pathogens) that accumulates in the cytoplasm and nucleus of cells (7, 8). There are numerous DNA sensors including: toll like receptor (TLR9), cGAS, the PYHIN family members AIM2 and IFI16, DExD/H box NA helicases (DDX41), DEAH-Box Helicases (DHX9/36) and ZBP1 (7). Several sensors including cGAS, DHX9, DHX36, DDX41, ZBP1 and IFI16 once activated by DNA converge on the adaptor protein STING leading to activation of the type I Interferon (IFN) response (7). In contrast, only the PYHIN family members IFI16 and AIM2 can activate the inflammasome (9, 10), a pro-inflammatory cytoplasmic multimeric protein complex that triggers the maturation of IL-1β and IL-18 via activation of caspase-1. Interestingly several studies report increased levels of circulating self and microbial DNA in patients with UC and CD. There are elevated levels of serum mtDNA (11), and increased total bacterial DNA (bactDNA) in blood and intestinal tissue of patients with active UC and CD (12). Blood bactDNA was also determined as a risk factor for relapse in a CD cohort (13). In addition, an elevated type I IFN signature in IBD has previously been described (14), and has also been associated with resistance to anti-TNFs (15). Overall, these observations suggest a possible scenario whereby alterations to DNA homeostasis may increase the activity of DNA sensors, promoting type I IFN signalling in UC.



Downloaded from journals.physiology.org/journal/ajpgi at Univ Col Cork (143.239.045.011) on October 3, 2022.

Inflammasome activation results in increased levels of inflammatory cytokines, can trigger cell death in different cell types and has been implicated in IBD immunopathogenesis, with most studies to date conducted in mice. The NLRP3 inflammasome was initially shown to promote intestinal inflammation, with mice lacking NLRP3 being protected from dextran sodium sulphate (DSS)-induced colitis (16). However, there is significant evidence that NLRP3 is protective, helping to maintain microbiota tolerance and preventing disruption of the epithelium (17, 18). Similarly, mice deficient for the PYHIN family and inflammasome activating DNA sensor AIM2 have increased susceptibility to DSS colitis (19). Increased levels of intestinal epithelial cell death is a characteristic of IBD immunopathogenesis and contributes to breakdown in gut barrier function (20) however the mechanisms underpinning this cell death are still not clear. DNA sensors, their downstream signalling components and inflammasomes regulate multiple cell death pathways. For example, the inflammasome activates pyroptosis via Gasdermin D and type I IFNs promote necroptosis via RIPK3-MLKL (21-23). Both are lytic forms of cell death that promote inflammation and protect against infection. ZBP1 is also known as a central regulator of PANoptosis; the simultaneous activation of apoptosis, pyroptosis, and necroptosis (23). Therefore, while it is clear that co-operation and crosstalk between various DNA sensor pathways, inflammasomes and type I IFN signalling can influence cell death decisions (24) the relative contribution of these mechanisms to increased epithelial cell death in IBD is unknown.

The reported increased presence of DNA ligands in IBD may promote DNA sensor activation. While DNA sensor signalling regulates critical aspects of intestinal homeostasis and inflammation; its role in IBD immunopathogenesis is not fully understood. This prompted us to investigate PRR and DNA signalling in colonic mucosal biopsy tissue from patients with UC and CD. We report an increase in expression of multiple DNA sensors, inflammasome components and the type I IFN response pathway in patients with active UC with clear evidence of cell type specific expression of PYHIN family members. We also found that treatment of human colonic organoids and macrophages with IFN partially mimics this transcriptional signature. In addition, treatment of human colonic organoids with IFN-β and



Downloaded from journals.physiology.org/journal/ajpgi at Univ Col Cork (143.239.045.011) on October 3, 2022.

141 TNF-α induces a novel form of epithelial cell death accompanied by release of IL-1β/IL-18.
142 In conclusion, we propose that increased activity of DNA sensor pathways and type I IFN
143 signalling may promote epithelial tissue damage, amplify inflammation and contribute to
144 pathogenesis in UC.
145



Downloaded from journals.physiology.org/journal/ajpgi at Univ Col Cork (143.239.045.011) on October 3, 2022.

## 2 Materials and Methods

### 2.1 Patient Cohort and Ethical Considerations

Colonic mucosal biopsies were collected from consented non-IBD patients and patients with IBD undergoing routine colonoscopy as part of standard of care. Ethical approval was obtained from the Clinical Research Ethics Committee of the Cork Teaching Hospitals (CREC). Informed consent was obtained from all patients in agreement with the Declaration of Helsinki. A total of 111 subjects were recruited, including patients with active UC, inactive UC, active CD, inactive CD and non-IBD controls (Table 1 and 2). All IBD patients had a confirmed diagnosis based on histopathological findings. Active and inactive disease were differentiated by the attending physician based on endoscopic and histological criteria. Endoscopic criteria included the absence of ulceration, granularity and friability, as well as the presence of normal vasculature. Histological criteria included the absence of detectable inflammation. Inactive patients were defined as being asymptomatic and having no signs of abnormality during endoscopy (which was carried out for surveillance reasons). Patient disease severity was not scored, as the research question only called for a comparison between active and inactive disease, correlation with severity was not required. Non-IBD controls were comprised of volunteers undergoing investigation of symptoms such as weight loss, anemia or altered bowel habit. A criterion for inclusion was normal histology on colonic biopsy.

### 2.2 Patient Samples and Processing

Preparation for colonoscopy consisted of administration of a single Fleet's enema one hour prior to the procedure. Volunteers were then placed in the left lateral position and endoscopy performed with a flexible video-colonoscope. All colonic mucosal biopsies were processed immediately. For RNA isolation, a single biopsy was stored overnight in RNAlater at 4°C. The biopsy was then placed in fresh RNAlater and stored at -80°C. For overnight cultures and immunohistochemistry patient biopsies were collected directly into collection media (DMEM media supplemented with 10 % FCS, penicillin/streptomycin, gentamycin, and



Downloaded from journals.physiology.org/journal/ajpgi at Univ Col Cork (143.239.045.011) on October 3, 2022.

amphotericin B) and transported to the research labs within 2-3 hours. Individual biopsies were placed in a well of a 24-well cell culture plate and incubated in collection media alone, with carrier control (DMSO) or inhibitors (caspase-1 inhibitor VX-765 (Selleckchem, S2228) and NLRP3 inhibitor MCC950 (R&D Systems, 5479)) at concentrations indicated in figure legends at 37 °C for 24 hours. After 24 hours aliquots of the tissue culture supernatants were removed and centrifuged at 250 x g for 5 minutes. The supernatants were then stored at –80 °C. Later the supernatants were analyzed by electrochemiluminescence for secretion of selected inflammatory mediators as per the manufacturer's instructions (Meso Scale Discovery). For normalization, after supernatant collection biopsies were removed and homogenized using Pierce™ T-PER tissue protein extraction reagent, and protein concentration was measured using the Pierce™ BCA protein assay kit. Details of the patient cohorts used for the overnight culture experiments can found in Table S1 (inhibitor experiments) and S2 (IBD cytokines).

To process biopsies for immunohistochemistry, a single biopsy was transferred from the collection tube, into a tube containing 4% paraformaldehyde (PFA). The sample was incubated overnight at 4°C. The biopsy was then cryoprotected by overnight perfusion in a 30% sucrose/PBS solution. The biopsy was removed from the sucrose solution and stored at -80 °C until processed for immunohistochemistry. Details of the patients whose biopsies were used for immunohistochemistry can be found in Table S2.

**2.3 Human Colonic Organoid Experiments**

Colonic mucosal biopsies from non-IBD individuals were obtained from adult patients at Cork University Hospital and Mercy University Hospital (Table S3). Protocols for crypt isolation and organoid culture were adapted from previously described methods (25-27), and are published previously (28, 29). Preparation of L-WRN conditioned media for organoid maintenance was performed as previously described (30). Before processing, biopsies were stored in Collection Medium (advanced DMEM/F12 (Gibco) supplemented with 10% FBS, 100 U/mL penicillin, 0.1 mg/mL streptomycin, 10 mM HEPES (Gibco), 2 mM Glutamax



Downloaded from journals.physiology.org/journal/ajpgi at Univ Col Cork (143.239.045.011) on October 3, 2022.

(Gibco), 1 × Amphotericin B (HyClone) and 100 µg/mL gentamicin (Sigma-Aldrich)). For processing, biopsies were washed in cold PBS supplemented with 1 × Amphotericin B and 100 µg/mL gentamicin. Washed biopsies were dissociated with Gentle Cell Dissociation Reagent (Stem Cell Technologies) containing 1 × Amphotericin B and 200 µg/mL Gentamicin for 20 min at room temperature with shaking at 180 rpm. Reagent activity was quenched with cold Wash Medium (Advanced DMEM/F12 supplemented with 10% FBS, 100 U/mL penicillin, 0.1 mg/mL streptomycin, 10 mM HEPES and 2 mM Glutamax), and passed through a 70 µm filter. The filtered solution was centrifuged for 5 min at 200 rcf and supernatant was discarded. The pellet was resuspended in Wash Medium, transferred to a 1.5 mL tube and centrifuged for 3 min at 400 rcf. Supernatant was removed and the pellet containing isolated crypts was resuspended in Reduced Growth Factor Type 2 BME (AMS Biotechnology). For 48-well plates, 20 µL domes of crypt/BME solution were seeded per well and plates were transferred into a cell culture incubator for 20 min. Once polymerised, the domes were overlaid with 300 µL of Proliferation Medium. Proliferation Medium was prepared as follows: Serum Free Medium (Advanced DMEM/F12 supplemented with 10 mM HEPES, 2 mM Glutamax, 1 × N2 supplement (Invitrogen), 1 × B27 supplement (Invitrogen), 1 mM N-acetylcysteine (Sigma-Aldrich) and 50 ng/mL human recombinant EGF (PeproTech)) was mixed 1:1 with L-WRN conditioned medium. This 50% L-WRN medium was supplemented with 10 mM nicotinamide (Sigma-Aldrich), 10 µM Y-27632 (Selleckchem), 10 µM SB-202190 (Sigma-Aldrich), 5 µM CHIR-99021 (Sigma-Aldrich) and 500 nM A-83-01 (Sigma-Aldrich). Proliferation Medium was replenished twice a week. For passaging, organoids were removed from BME and dissociated with TrypLE Express (Gibco) supplemented with 10 µM Y-27632, which was then quenched with Wash Medium. The cell solution was centrifuged for 3 min at 400 rcf and supernatant removed. The pellet was resuspended in fresh BME and seeded. Passaging was performed every 1–2 weeks, using a 1:3 split ratio. For RNA extraction experiments organoids were seeded in 48-well plates. For viability assays and supernatant analysis organoids were seeded in 96-well plates at 0.2 x $10^5$ cells/well. For undifferentiated organoid experiments, the organoids were left to recover



Downloaded from journals.physiology.org/journal/ajpgi at Univ Col Cork (143.239.045.011) on October 3, 2022.

for 3 days and treated as indicated in the figures and figure legends. For differentiation experiments, organoids were left to recover in Proliferation Media overnight following seeding. They were then switched to Differentiation Media, which contains only 5% L-WRN medium (95% Serum Free Medium) and without nicotinamide, SB-202190 or CHIR 99021. Organoids were differentiated for 3 days for RNA isolation and 2 days for viability/Meso Scale Discovery (MSD) experiments followed by treatments as indicated in the figures and figure legends. For treatments all cytokines used were from Peprotech, tofacitinib was from Sigma-Merk (PZ0017), MCC950 and VX-765 from Selleckchem (S7809 and S2228), Z-VAD-FMK from Cayman Chemical (14463) and Z-IETD-FMK from R&D Systems (FMK007). Organoid supernatants were collected and used fresh for cytokine/chemokine analysis by electrochemiluminescence U-Plex assay per the manufacturer's instructions (MSD). Organoid viability was determined using CellTiter-Glo® 3D (Promega) per the manufacturer's instructions. Phase contrast and fluorescence microscopy images were acquired using the EVOS XL Core Cell Imaging System (Invitrogen). Image processing was done using ImageJ-win64 software.

**2.4 Human primary macrophage experiment**

$CD14^{+ve}$ monocytes were isolated by positive selection with anti-CD14 beads (Miltenyi Biotec) from peripheral blood mononuclear cells provided by Irish Blood Transfusion Service. Monocytes were seeded in 96-well plates at $0.1 \times 10^6$ cells/well. Monocytes were cultured in RPMI1640 medium (Sigma-Merk) supplemented with 10% FBS, 100 U/mL penicillin, 0.1 mg/mL streptomycin, and 10 ng/mL M-CSF (Peprotech) for five days to allow differentiation into macrophages. Macrophages were treated with human recombinant cytokines (R&D Systems) as indicated in the figures and figure legends.

**2.5 RNA isolation and gene expression analysis**

Colonic mucosal biopsies preserved in RNALater were added to Magnalyser tubes containing ceramic beads (Roche) with 600 µL *mir*Vana lysis buffer (Ambion) and



Downloaded from journals.physiology.org/journal/ajpgi at Univ Col Cork (143.239.045.011) on October 3, 2022.

homogenised using the MagNA Lyser Instrument (Roche). Lysates were centrifuged to pellet the debris and the supernatant was collected. 300 µL of the lysate was processed for RNA isolation. Total RNA was isolated from samples using the *mir*Vana miRNA Isolation Kit (Ambion) according to the manufacturer's instructions. All biopsy RNA was DNase treated, except for RNA samples from the initial PRR screen (Fig. 1a). RNA was used immediately or frozen at -80°C for later use. After treatment, organoids were washed twice with cold PBS and re-suspended in 300 µL of organoid harvesting solution (Cultrex). Domes were disrupted and transferred to 1.5 mL tubes. After a 1 hour incubation at 4°C with rocking at 180 rpm, organoids were centrifuged, washed twice in cold PBS and the pellet was re-suspended in 350 µL of RLT buffer (Qiagen). Macrophage RNA was collected by adding 350 µl lysis buffer per well directly to the cell culture plate after treatment. Lysates were stored at -80°C until RNA extraction. For organoid and macrophage lysates, RNA extraction was performed using the RNeasy Micro Kit with on-column DNase-digestion, following the manufacturer's instructions (Qiagen). RNA was frozen at -80°C for later use. cDNA was synthesised with 100 ng of RNA using Transcriptor Reverse Transcriptase (Roche) and random hexamer primers. RT-qPCR was performed in the LightCycler® 480 instrument (Roche). The 51 genes in the PRR screen assays were purchased as a RealTime ready Custom Panel (Roche), the other primers were purchased from Eurofins Genomics and combined with complementary Universal ProbeLibrary probes (Roche) or TaqMan assays were used (Table S4). In addition, the following RealTime ready assays were purchased from Roche: HPRT1 (cat# 102079) and RPL13A (cat# 102119). For biopsy samples gene expression was quantified relative to β-actin (*ACTB*) and TATA-binding protein (*TBP*), using the $2^{-\Delta\Delta Ct}$ method (31) in comparison to a pooled biopsy calibrator control. Relative gene expression was calculated using the $2^{-\Delta\Delta Ct}$ method and normalised to the geometric mean of Hypoxanthine Phosphoribosyltransferase 1 *(HPRT1*) and Ribosomal Protein L13a (*RPL13A*) for organoid samples (determined by geNorm analysis using qbase software, https://www.qbaseplus.com/) and *ACTB* for macrophages.



Downloaded from journals.physiology.org/journal/ajpgi at Univ Col Cork (143.239.045.011) on October 3, 2022.

**2.6 Immunohistochemistry**

Biopsies stored at -80$^{O}$C were mounted in Optimal Cutting Temperature (OCT) tissue-freezing medium (Tissue Tek) and sectioned at 10 µm using a cyrostat. Samples were blocked with 3% $H_2O_2$ in distilled water for 20 minutes. Slides were incubated with primary antibody overnight at 4°C. The primary antibodies tested were ZBP1 (13285-1-AP, Proteintech) and IFI16 (sc-8023 Santa Cruz Biotechnology). For the working concentrations the ZBP1 antibody was diluted 1:100 and the IFI16 antibody 1:1000. Antibody binding was localized using a biotinylated secondary antibody (2.5 ug/mL working concentration), avidin-conjugated HRP and DAB substrate, contained within the Vectastain ABC detection kit (Vector Laboratories). Slides were counterstained with hematoxylin. Samples were imaged using an Olympus BX61 and 40x objective lens.

**2.7 Primary isolated epithelial cell preparation**

Primary human epithelial cells were isolated from surgical specimens as previously described (32). The epithelial cell fractions were depleted of leucocytes by treatment with anti-CD45 charged paramagnetic beads. Purified cells were washed in RNase-free phosphate buffered saline and stored at -80°C. Samples were collected after patients' written, informed consent. The study was approved by the Local Ethics Research Committee of the Medical Faculty, Umeå University, Umeå, Sweden (Registration numbers: 03-477 and 03-503). Patient characteristics are summarised in Supplementary Table S5.

**2.8 Single cell RNA-Seq bioinformatics and data visualisation**

Single cell data from Smillie *et al.* 2019 (33) was obtained from the Broad Institute single cell portal (https://singlecell.broadinstitute.org/single_cell). Seurat (34) running in R (R Core Team (2020). R: A language and environment for statistical computing. R Foundation for Statistical Computing, Vienna, Austria. https://www.R-project.org/) was used to generate objects for the epithelial and immune cell-gene matrices from the publicly available cell-gene matrices and meta data files. Seurat's AddModuleScore was used to compute the



Downloaded from journals.physiology.org/journal/ajpgi at Univ Col Cork (143.239.045.011) on October 3, 2022.

314 expression of individual genes. Figures were produced using ggplot2 (35) and color scales
315 for gene expression produced using the turbo colour scale from the viridis package (36).
316
317 **2.9 Statistical analysis**
318 Graphs and statistical analysis were produced via GraphPad Prism® software. Statistical
319 tests used for each experiment are described in the figure legends. Statistical significance
320 was defined as a p-value less than 0.05. The heatmap from Figure 1 was generated using
321 Genesis software (37). In Genesis, the data were used to generate an expression matrix,
322 and then visualized using the “Expression image: difference” setting. Hierarchical clustering
323 was performed using the “average linkage WPGMA” agglomeration rule (Weighted pair-
324 group average linkage), for calculation parameters samples were clustered by gene.
325



Downloaded from journals.physiology.org/journal/ajpgi at Univ Col Cork (143.239.045.011) on October 3, 2022.

## 3 RESULTS

### 3.1 Upregulated cluster of PRR genes in active UC includes DNA sensors

We performed a comprehensive review of PRR literature to select a panel of known human TLRs, C-type Lectin Receptors (CLRs), NOD-Like Receptors (NLRs) and RIG-Like Receptors (RLRs). PRRs can be broadly classified into transmembrane receptors, including TLRs and CLRs which are located at the cell membrane or in intracellular membrane bound structures, and cytosolic receptors like the NLRs and RLRs. We carried out a gene expression screen for these 51 PRRs on an initial cohort (cohort 1) of colonic biopsies of non-IBD subjects and patients with IBD from active/inactive sites (Table 1) (Fig. 1a). Nine PRR genes (*CLEC1B*, *CLEC12B*, *NLRP4*, *NLRP5*, *NLRP7*, *NLRP8*, *NLRP9*, *NLRP10*, *NLRP13*) were undetectable in all samples and excluded from the analysis. After hierarchical clustering, a cluster of genes was observed that had increased expression in active UC when compared to either inactive or non-IBD control tissue (Fig. 1a). This cluster contained NLRs (class II major histocompatibility complex transactivator (*CIITA*), NLR family pyrin domain containing 1 (*NLRP1*), NLR family pyrin domain containing 14 (*NLRP14*)), one CLR (C-type lectin domain containing 5A (*CLEC5A*)), one TLR (toll like receptor 9 (*TLR9*)) and two cytosolic DNA sensors (absent in melanoma 2 (*AIM2*), Z-DNA binding protein 1 (*ZBP1*)). We did not detect expression of *CLEC5A* in the non-IBD group and so we removed it from our analysis. There was a significant increase in *CIITA* and *NLRP*1 in active UC when compared to non-IBD controls (Fig. 1b). Expression of the DNA sensors *AIM2* and *ZBP1* and a putative negative regulator of cytosolic nucleic acid sensing *NLRP14* (38) were significantly increased in active UC compared to both inactive UC and non-IBD tissue (Fig. 1b). This expression pattern was not seen in CD.

It's important to note that female patients were overrepresented in the active CD group (7 females to 1 male). Gender specific effects in IBD are well recognized, and can influence multiple factors including epidemiology, risk associated with susceptibility gene variants, disease activity and phenotype, disease complications, response to biologics and prevalence of depression (37). This overrepresentation of female patients in our CD cohort



Downloaded from journals.physiology.org/journal/ajpgi at Univ Col Cork (143.239.045.011) on October 3, 2022.

may have affected our results. As the increase in cytosolic DNA sensor expression was significant only in active UC and not in inactive UC or CD samples, we decided to investigate DNA recognition and associated pathways in UC.

**3.2 PYHIN family signalling and canonical inflammasome activation are increased in active UC**

The PYHIN family consists of AIM2, IFI16, PYHIN1, MNDA and POP3. AIM2 and IFI16 can activate the inflammasome after directly binding to DNA (Fig. 2a). To validate the increase in *AIM2* expression we observed in the PRR screen, we investigated the expression of the PYHIN family members in an extended cohort of non-IBD patients and patients with UC (cohort 2). These patients belong to a second cohort recruited after the PRR screen was performed and added to cohort 1 (Table 2). To confirm the status of the inflamed samples we detected increased expression of the Th1 cytokines interferon gamma (*IFNG*) and tumor necrosis factor (*TNF*) in active UC compared to non-IBD control biopsies (Fig. S1a) and increased secretion of IFN-γ, TNF-α, IL-6 and IL-10 from overnight cultures of active UC biopsies compared to non-IBD and inactive UC biopsies (Fig. S1b). Expression of the inflammasome sensors *AIM2* and *IFI16* were significantly increased in active UC biopsies when compared to control (Fig. 2b). *AIM2* gene expression was significantly increased in active UC biopsies when compared to inactive samples. Pyrin and HIN domain family member 1 (*PYHIN1*) and myeloid cell nuclear differentiation antigen (*MNDA*) were significantly increased in expression in both active and inactive UC biopsy samples compared to control (Fig. 2b). In contrast, the expression of the endosome localized transmembrane DNA sensor *TLR9* was significantly higher in inactive UC samples compared to active UC samples and controls (Fig. S1a). Using purified patient derived primary enterocytes (IECs) we confirmed by RT-qPCR a non-significant increased expression of *IFI16* from patients with UC when compared with non-IBD controls (Table S5).

Next, we investigated the expression and cellular distribution of IFI16 protein by immunohistochemistry in colonic mucosal biopsies from non-IBD control and UC patients.



Downloaded from journals.physiology.org/journal/ajpgi at Univ Col Cork (143.239.045.011) on October 3, 2022.

IFI16 protein was seen in the lamina propria (LP) and epithelial cells of all samples (Fig. 2c). Increased staining of IFI16 in cells was seen in the active and inactive UC samples compared to controls (Fig. 2c). Additionally, positive cells directly underlying the epithelial monolayer were observed in UC tissue (Fig. 2c iv & v). Similarly, an increased IFI16 staining in LP was seen in active UC. Strong epithelial expression was seen in all cells of the crypts of active UC, sub-cellular distribution was primarily nuclear with some evidence of cytoplasmic localisation (Fig. 2c iv).

We assayed for additional components of DNA sensor inflammasomes including the effector protease pro-caspase-1 and the target cytokines, IL-1β and IL-18. Caspase 1 (*CASP1*) expression was significantly upregulated in UC tissue when compared to the control group, and expression was increased in active compared to inactive UC (Fig. 2d). Significantly increased expression of interleukin 1 beta (*IL1B*) and interleukin 18 (*IL18*) was seen in UC tissue when compared to non-IBD controls, as well as the IL-1 family member interleukin 33 (*IL33*) (Fig. 2d). The role of the NLRP3 inflammasome in regulating intestinal inflammation in mice has been reported. However, in our initial PRR screen we found no change in expression of NLR family pyrin domain containing 3 (*NLRP3*) in active UC compared to non-IBD controls (Fig. S1a). Considering the established role of gender-based differences in IBD (39), we compared the expression of all genes assayed in biopsies between males and females in the non-IBD, active UC and inactive UC patient groups. We found a significant increase in *CASP1* expression for female patients in the active UC group and a significant decrease in expression of *IFI16* in female patients in the inactive UC group (Fig. S1c). Although these are intriguing findings, a much larger patient cohort would be required to confirm these observations.

We checked if the elevated gene expression of inflammasome components was associated with increased secretion of IL-1β protein from active UC tissue. We confirmed that IL-1β secretion was increased in active UC compared to non-IBD control using *ex-vivo* overnight biopsy cultures (Fig. S1b). To investigate if the NLRP3 inflammasome sensor was contributing to enhanced production of IL-1β, we treated biopsy cultures with the selective



Downloaded from journals.physiology.org/journal/ajpgi at Univ Col Cork (143.239.045.011) on October 3, 2022.

NLRP3 inhibitor MCC950 and the selective caspase-1 inhibitor VX-765. IL-1β production was significantly reduced in active biopsies that were treated with VX-765 and MCC950, however VX-765 had a greater inhibitory effect (Fig. 2e). After normalizing the data, expressing each data point as fold change of matching DMSO control per patient, we found the difference between VX-765 and MCC950 groups was significant (Fig. S1e). The production of IL-1RA – while not reaching statistical significance – was reduced in VX-765 treated UC biopsies. There was a non-significant increase in the IL-1RA/IL-1β ratio (Fig. 2e), a lowered IL-1RA/IL-1β ratio has previously been associated with disease severity in IBD (40). Overall, the data show upregulation of canonical PYHIN inflammasome member components and signalling in active UC biopsy tissue, and that IL-1β release is largely dependent on inflammasome activation. Further, the data suggest that IL-1β production may only be partially dependent on NLRP3 activity. However, this observation would require a dose response experiment to confirm. Nonetheless, the $IC_{50}$ for MCC950 in human immune cell types is in the low nM range (41), so it is probable that the 10 μM dose of MCC950 we used for colonic mucosal biopsy tissue experiments would have maximal inhibition.

### 3.3 *IFI16* expression is increased in multiple epithelial and immune cell lineages in active UC

Colonic mucosal biopsies consist of a complex mixture of cell populations including epithelial, stromal and immune cell lineages. When using whole biopsy tissue for expression studies, it's impossible to accurately assess the contributions of the various populations to the transcriptional profile. With this in mind, we decided to investigate the cell type specific expression of the differentially expressed PYHIN family genes we identified using a publicly available UC single cell RNA-Seq dataset (33). In their paper, Smillie *et al*. reported a single cell gene expression atlas of 366,650 cells isolated from the colonic mucosa of patients with inactive and active UC and healthy individuals (33). They clustered the single cell profiles from all samples and annotated each cluster using expression of known cell markers,



Downloaded from journals.physiology.org/journal/ajpgi at Univ Col Cork (143.239.045.011) on October 3, 2022.

identifying 15 epithelial and 23 immune cell lineages (Fig. 3a & b). For our analysis, we projected the expression of our genes of interest over the t-SNE plots of the epithelial and immune cell populations (Fig. 3c & d).

*AIM2* expression was very sporadic in the epithelial populations, with only a few positive cells detected across all states (Fig. 3c). A similar profile was seen for the other PYHIN family genes *PYHIN1* and *MNDA* (Fig. S2c). For immune cells, *AIM2* expression was increased in cycling B and T cells in active UC, and expression can be seen in plasma cells and macrophages across all states (Fig. 3d). *PYHIN1* expression was increased in T regulatory cells (Tregs), $CD8^+$ LP and natural killer (NK) cells in active and inactive UC (Fig. S2d). *MNDA* was highly expressed by inflammatory monocytes, a cell type present only in active and inactive UC samples. Like the other PYHIN genes, *IFI16* expression was sporadic in healthy epithelial cells. However, expression dramatically increased in active and inactive UC across multiple epithelial cell lineages, including stem cells, transit amplifying (TA) cells, Best4+ enterocytes and immature goblet cells (Fig. 3c). There was a small cluster of enterocytes in active UC that highly expressed *IFI16*. For immune cell populations, *IFI16* expression was increased in cycling B cells, cycling T cells, macrophages and inflammatory monocytes from active and inactive UC (Fig. 4d). There was an increase in expression of the inflammasome effector *CASP1* in epithelial TA cells for active and inactive UC (Fig. 4c). The same small group of *IFI16*+ enterocytes in active UC were also positive for *CASP1*. Inflammatory monocytes and macrophages expressed *CASP1* at high levels (Fig. 3d).

As anticipated, this analysis helped us understand which cell types are likely responsible for the increase in *PYHIN* family gene and *CASP1* expression we observed in whole biopsy tissue. The PYHIN family members *AIM2*, *PYHIN1* and *MNDA* are expressed at very low levels and sporadically in epithelial cell populations for all states. *IFI16* expression is inconsistent in healthy epithelial samples, but is dramatically increased in undifferentiated, adsorptive and secretory cell lineages of active UC. Expression of *AIM2* and *PYHIN1* is increased in lymphoid immune lineages from UC samples. Inflammatory



Downloaded from journals.physiology.org/journal/ajpgi at Univ Col Cork (143.239.045.011) on October 3, 2022.

monocytes, one of the primary cell types responsible for driving inflammation in UC, express *MNDA*, *IFI16* and *CASP1* at high levels.

### 3.4 DNA sensors, STING dependent signalling and type I IFN signalling are upregulated in active UC

Increased expression of *ZBP1* in active UC biopsies from our initial screen (Fig. 1b) prompted us to analyse in greater detail the expression of DNA sensors and STING signalling pathway components that regulate type I IFN signalling (Fig. 4a). *ZBP1* and cyclic GMP-AMP synthase (*cGAS*) expression were significantly upregulated in active UC biopsies when compared to control or inactive UC biopsies (Fig. 4b). DEAD-box helicase 41 (*DDX41*) had elevated expression in both active and inactive UC tissue compared to controls (Fig. S1f). There was increased expression in active UC of the DNA sensor DExH-box helicase 9 (*DHX9*), but no change in DEAH-box helicase 36 (*DHX36*) (Fig. S1f).

Next, we examined the expression and distribution of ZBP1 protein in non-IBD control and UC patients using immunohistochemistry. A diffuse positive staining for ZBP1 in discrete LP cells was seen in the non-IBD control (Fig. 4c ii). Inactive UC biopsies had a similar distribution of ZBP1 expression, in addition to ZBP1 positive cells underlying the crypt epithelial monolayer (Fig. 4c iii & iv). There was an increased staining of ZBP1 in LP cells in active UC (Fig. 4c v & vi), while the luminal surface epithelium of non-IBD and UC samples was positive for ZBP1 (Fig. S1g). Several ZBP1 positive epithelial cells were also seen in the crypts of inflamed tissue from UC patients (Fig. 4c vi).

We next assayed the expression of the signalling adapter protein STING, its target kinase TBK1 and the transcription factor IRF3. Stimulator of interferon response cGAMP interactor 1 (*STING*) expression was found to be significantly upregulated in active UC samples when compared to non-IBD controls (Fig. 4d). Downstream of STING there was a significant upregulation of both TANK binding kinase 1 (*TBK1)* and interferon regulatory factor 3 (*IRF3)* expression in active and inactive UC compared to control samples (Fig. 4d & e). Expression of the transcription factor interferon regulatory factor 7 (*IRF7*), which is



Downloaded from journals.physiology.org/journal/ajpgi at Univ Col Cork (143.239.045.011) on October 3, 2022.

activated by the transmembrane DNA sensor TLR9, the DNA sensor DHX36 and regulated by the PYHIN family member MNDA (42), was also increased in both active and inactive UC samples compared to controls (Fig. 4e). Phosphorylation of IRF3 and IRF7 leads to the induction of the type I IFNs, IFN-β and IFNα1, respectively. We found no change in interferon alpha 1 (*IFNA1*) expression between the patient groups (Fig. 4f). Interferon beta 1 (*IFNB1*) expression was significantly upregulated in both active and inactive UC patients (Fig. 4f). Variance among the active group of patients was substantial (SD of ±34.57 relative fold change), with 8 of 33 patients having less than 1-fold change and 9 of 33 patients having over 20-fold change in expression compared to the control group. This suggests there may be a high *IFNB1* expressing sub-population of active patients. However, we could not detect IFN-β in the supernatant of colonic explants (Fig. S1b). This could be due to transient low-level production and degradation of the secreted protein as detection of IFN-β protein in biological samples is known to be challenging.

To support findings suggesting that the type I IFN response was activated in the UC patient group, a panel of four direct type I IFN responsive biomarker target genes was investigated. The selection of the panel was based on previous publications that validated these genes as biomarkers for type I IFN response in human samples and investigated the expression of these genes in IBD (14, 43, 44). The panel contains four classic type I IFN induced antiviral genes: 2'-5'-oligoadenylate synthetase 2 (*OAS2*), interferon induced protein with tetratricopeptide repeats 2 (*IFIT2*), MX dynamin like GTPase 1 (*MX1*) and MX dynamin like GTPase 2 (*MX2*). OAS2 and IFIT2 expression were increased in active UC (Fig. 4g). A significant upregulation of MX2 was found in both active and inactive UC biopsy tissue. These data support elevated type I IFN signalling in active disease. Regarding gender effects, we found a modest but significant decrease in expression of *ZBP1*, *MX2* and *OAS2* for female patients in the inactive UC patient group (Fig. S1d).

Overall, the data suggest that there is an increase in DNA sensor activity, STING-TBK1-IRF3 axis signalling, IFN-β expression and type I IFN regulated gene expression in active UC colonic biopsies.



Downloaded from journals.physiology.org/journal/ajpgi at Univ Col Cork (143.239.045.011) on October 3, 2022.

519

520 **3.5 *STING* expression is increased in multiple epithelial cell lineages in active and**
521 **inactive UC**

522 Next, we analysed the expression of DNA sensors and the downstream adapter protein
523 STING - that induce type I IFNs - in the publicly available UC single cell atlas (Fig. 5). *ZBP1*
524 expression in the epithelium was inconsistent, except for a small cluster of positive
525 enterocytes only present in active UC (Fig. 5c). For immune populations, *ZBP1* expression
526 was increased in cycling B and T cells in active and inactive UC (Fig. 5d). There was also a
527 population of high expressing plasma cells present only in UC. For epithelial populations,
528 *cGAS* expression was increased in active and inactive UC epithelial TA cells (Fig. 5c). There
529 was an increase in *cGAS* expression in cycling B and T cells from active and inactive UC
530 samples (Fig. 5d). A cluster of *cGAS*+ inflammatory monocytes was present in active UC, a
531 cell type found only in active UC. *STING* expression was increased across multiple epithelial
532 cell lineages in UC, including stem cells, TA cells (cycling and secretory), immature
533 enterocytes and enterocytes (Fig. 5c). Interestingly, in both active and inactive UC there was
534 a small cluster of *STING* positive M cells, a highly specialized cell type responsible for
535 luminal sampling of microbes. Additionally, for inactive UC there was an increase in *STING*
536 positive immature goblet cells. For immune cells, both active and inactive UC samples
537 contained a cluster of *STING* positive inflammatory monocytes (Fig. 5d). There was also a
538 group of high expressing *STING* positive Tregs present in active and inactive UC, generally
539 considered an anti-inflammatory cell type. The *STING* target kinase *TBK1* had a similar
540 expression pattern to *STING* in epithelial cells for active and inactive UC samples (Fig. S2c).

541 The expression of the type I IFN regulating DNA sensors (*ZBP1*, *cGAS)* and the
542 adapter protein *STING* were increased in UC samples, which is consistent with our findings
543 from whole biopsy tissue. There was an increase in *ZBP1* and *cGAS* expression in the UC
544 epithelium, however this was restricted to enterocytes and TA cells respectively. Lymphoid



Downloaded from journals.physiology.org/journal/ajpgi at Univ Col Cork (143.239.045.011) on October 3, 2022.

545 immune lineages had increased expression of *ZBP1* and *cGAS* in active and inactive UC,
546 and there was a cluster of *cGAS*+ and *STING*+ inflammatory monocytes in active UC.
547 *STING* expression was increased in undifferentiated, adsorptive, secretory and M cells in
548 active and inactive UC, and these populations were also positive for the kinase *TBK1*.
549

550 **3.6 Type I IFN increases IFI16 and inflammasome gene expression in human colonic**
551 **organoids**

552 STING-induced type I IFN production and signalling can interact with and regulate the
553 expression and activity of the PYHIN inflammasomes (45). We hypothesised that the
554 increase in type I IFN response observed in patients with active UC could be driving the
555 elevated expression of PYHIN genes (Fig. 2b). We tested our hypothesis by examining the
556 transcriptional response of human non-IBD colonic epithelial organoids to IFN-β stimulation.
557 We also stimulated organoids with type II IFN (IFN-γ) and TNF-α, both of which are IBD
558 associated cytokines elevated in active UC overnight biopsy cultures (Fig. S1b). Like type I
559 IFNs, IFN-γ utilises JAK/STAT signalling downstream of its receptor, and TNF-α is known to
560 synergise with IFNs to increase transcription and induce cell death of intestinal epithelial
561 cells (28, 29).

562 We chose to focus on the epithelium due to our analysis of the single cell UC dataset
563 and our interest in the cytotoxic effects of IFNs on this cell type. We were intrigued by the
564 induction of IFI16 across multiple epithelial cell lineages in UC (stem, TA, adsorptive and
565 secretory cell types), and the relatively low expression of other PYHIN family members
566 across all states (AIM2, PYHIN1, MNDA) (Fig. 3c). As IFI16 expression was increased in
567 various epithelial cell lineages, we compared the response between undifferentiated
568 (enriched for stem cells and TA cells) and differentiated (containing secretory and adsorptive
569 cells) organoids to IFN-γ and TNF-α (differentiated status was confirmed by the expression
570 of cell type specific marker genes and morphology (Fig. S3a & b)). Unlike epithelial cells,



Downloaded from journals.physiology.org/journal/ajpgi at Univ Col Cork (143.239.045.011) on October 3, 2022.

571 macrophages and inflammatory monocytes were high expressors of several PYHIN family
572 genes in both healthy and UC states (Fig. 3d). Considering this, we decided to also examine
573 expression of PYHIN members in primary human monocyte derived macrophages activated
574 by IFN-γ.

575 A sub-population of organoids treated with IFN-β or IFN-γ in combination with TNF-α
576 displayed morphological evidence of cell death (Fig. 6a), including disruption of epithelial
577 integrity and membrane blebbing. These features were not seen in organoids treated with
578 IFN-β or IFN-γ alone (Fig. 6a). *IFI16* was the only PYHIN family member that was detectable
579 in organoids (Fig. 6b), which matched the data from directly isolated primary IECs and
580 analysis of epithelial cell types in the single cell UC dataset (Table S5 and Fig. 3c). *IFI16*
581 expression was detectable in unstimulated organoids and was significantly upregulated by
582 IFN-β treatment (Fig. 6b). A similar response was seen in differentiated organoids co-treated
583 with IFN-γ and TNF-α (Fig. S4a), and in HT-29 colon cancer cells treated with type I IFNs
584 (Fig. S4b). By comparison, in macrophages all four PYHIN sensors were detected in
585 untreated cells, and both *AIM2* and *IFI16* were significantly upregulated in response to IFN-γ
586 stimulation (Fig. S4c). This is consistent with the analysis of the single cell dataset, where
587 *AIM2*, *IFI16* and *MNDA* were highly expressed by macrophages and inflammatory
588 monocytes (Fig. 3d). In organoids detection of *NLRP3* was inconsistent and there was no
589 significant increase in expression after cytokine treatment (Fig. 6b and Fig. S4a and c).
590 *NLRP3* was not detected in directly isolated primary IECs from non-IBD control and active
591 UC samples (Table S5), supporting our findings in the organoids.

592 Next, we investigated the expression of canonical inflammasome pathway
593 components downstream of inflammasome sensors. *CASP1* expression was upregulated in
594 response to IFN-β and IFN-γ treatment (Fig. 6c). Increase in *IL1B* expression required co-
595 treatment with TNF-α for both IFN-β and IFN-γ. Differentiation of organoids increased
596 *CASP1* and *IL1B* expression in response to IFN-γ and TNF-α co-treatment (Fig. S4d).
597 Differentiation increased expression of *IL18* at baseline, which agrees with the known



Downloaded from journals.physiology.org/journal/ajpgi at Univ Col Cork (143.239.045.011) on October 3, 2022.

598 constitutive expression of *IL18* by intestinal epithelial cells (46). *CASP1* expression was
599 increased in IFN-γ treated macrophages, but there was no evidence of *IL1B* induction and
600 *IL18* expression was reduced (Fig. S4e).

601 In summary, the cell type dependent expression pattern for PYHIN family genes
602 observed in the UC single cell dataset was recapitulated in primary human epithelial
603 organoid and macrophages cultures. In addition, non-IBD human colonic organoids
604 stimulated with IFN-β showed increased expression of *IFI16* and downstream inflammasome
605 components required for IL-1β processing; and this gene signature was enhanced by co-
606 treatment with TNF-α.

607

608 **3.7 Type I IFN increases ZBP1-STING expression in human colonic organoids**

609 Positive feedback regulation between type I IFN and cGAS/ZBP1-STING has been
610 demonstrated previously (22, 47). This prompted us to investigate if IFN-β treatment could
611 increase the expression of type I IFN regulating DNA sensors and STING signalling
612 components in organoids. IFN-β significantly upregulated the expression of *ZBP1* in
613 organoids (Fig. 7a). *cGAS* expression was increased in organoids only when co-treated with
614 IFN-γ or IFN-β and TNF-α. Differentiation of organoids increased *ZBP1* and *cGAS*
615 expression in response to IFN-γ and TNF-α co-treatment (Fig. S5a). This observation is
616 supported by our analysis of the single cell dataset, where expression of *ZBP1* was highest
617 in active UC enterocytes (Fig. 5c). Type I IFNs also increased expression of *ZBP1* and
618 *cGAS* in HT-29 cells (Fig. S5b). In contrast, *ZBP1* was not detected in unstimulated primary
619 macrophages, and there was only a slight insignificant increase in expression with IFN-γ
620 treatment (Fig. S5c). However, IFN-γ treatment did increase *cGAS* expression in
621 macrophages (Fig. S5c), this aligns with the single cell dataset where a cluster of *cGAS*+
622 inflammatory monocytes was present in active UC (Fig. 5d).

623 We examined signalling components downstream of the DNA sensors and found
624 there was increased expression of *STING* that was IFN-β dependent in organoids (Fig. 7b).



Downloaded from journals.physiology.org/journal/ajpgi at Univ Col Cork (143.239.045.011) on October 3, 2022.

Organoid differentiation significantly increased expression of *STING* and *TBK1* following co-treatment with IFN-γ and TNF-α (Fig. S5a). There was no change in expression of STING signalling components in macrophages after IFN-γ treatment (Fig. S5c). When we examined the expression of type I IFN responsive biomarker interferon stimulated genes (ISGs) (Fig. 7c), there was an increased expression of *IFIT2*, *MX1* and *MX2* only in IFN-β treated organoids. We also examined expression of guanylate binding protein 1 (*GBP1)*, which is responsive to both type I and II IFN. As expected *GBP1* was induced by co-treatment with both IFN-β or IFN-γ and TNFα (Fig. 7c). This further validated the selection of this type I IFN response biomarker gene panel to characterise a functional and ongoing response to type I IFN in our patient biopsy cohort (Fig. 3g). In conclusion, treatment with type I IFN increased ZBP1-STING pathway expression in human colonic organoids.

**3.8 IFN-β and TNF-α co-treatment induces cell death and IL-1β/IL-18 secretion in organoids that are caspase independent**

We established that IFN-β or IFN-γ and TNF-α co-treatment upregulate the IFI16 inflammasome and ZBP1-STING pathways at the transcriptional level in primary colonic epithelial organoids. However, we wanted to determine if these treatments could induce secretion of IL-1β/IL-18 and IFN-β protein. Inflammasome and ZBP1 signalling can also activate pyroptosis and necroptosis (23), therefore we decided to examine organoid viability in parallel. This is relevant to the pathology of UC, as excessive epithelial cell death contributes to the breakdown of gut barrier function in active disease (48).

Knowing that differentiation of organoids increases transcriptional responsiveness to IFN-γ (Fig. S4a & d and S5a), we directly compared undifferentiated and differentiated organoids. In both states IFN-β or IFN-γ in combination with TNF-α reduced organoid viability vs untreated controls (Fig. 8a). Differentiation sensitised organoids to IFN-γ, and increased sensitivity to TNF-α treatment. These observations were confirmed by examination of organoid morphology using live microscopy (Fig. S6a).



Downloaded from journals.physiology.org/journal/ajpgi at Univ Col Cork (143.239.045.011) on October 3, 2022.

652 Studies have suggested that the microbiota is involved in constitutive IFN-β
653 production (49), however we detected IFN-β secretion in colonic organoids at baseline under
654 sterile conditions (Fig. S6b). IFN-γ and TNF-α treatment had no statistically significant effect
655 on IFN-β secretion. Organoid IL-1β levels at baseline were almost undetectable (Fig. 8b).
656 Treatment with IFN-β or IFN-γ in combination with TNF-α increased IL-1β release in both
657 undifferentiated and differentiated states. We could detect a small amount of IL-18 in
658 untreated organoids, which was increased after differentiation, supporting our IL-18 RT-
659 qPCR data (Fig. S4d). Differentiation significantly increased the levels of IL-18 for all
660 cytokine treatments compared to undifferentiated organoids (Fig. 8b). Treatment with IFN-β
661 or IFN-γ in combination with TNF-α induced the most IL-18 release in both organoid states.
662 We then conducted experiments to determine the mechanism responsible for driving
663 both cell death and the release of IL-1β/IL-18 from organoids by using small molecular
664 inhibitors to perturb regulators of cell death and canonical/non-canonical inflammasome
665 components (Fig. 8c & d). These included NLRP3 (MCC950), caspase-1/4 (VX-765) and
666 caspase-8 (Z-IETD-FMK). As both type I and II IFN signalling are driven by JAK activity, we
667 included tofacitinib a JAK1/3 inhibitor approved for the treatment of UC. We selected a 10
668 μM dose of tofacitinib because we previously found that loss of cell viability induced by IFN
669 in undifferentiated human colonic organoids could be significantly reduced with 1 μM, but
670 maximum rescue was at 10 μM (29). In healthy volunteers treated with doses of tofacitinib
671 approved for UC (one 10 mg tablet per day) serum $C_{max}$ levels for the drug were 312 nM
672 (50). However, it's possible that exposure to the drug at the mucosal surface of the colon
673 could be higher than in plasma. We conducted these experiments in differentiated organoids
674 only as they were most responsive to IFN-β/IFN-γ treatment.
675 Tofacitinib partially rescued the loss of viability induced by IFN-β or IFN-γ in
676 combination with TNF-α (Fig. 8c), approximately to the level of relative viability seen with
677 TNF-α treatment alone (Fig. 8a). The inflammasome inhibitors MCC990 and VX-765 did not
678 prevent loss of viability, excluding pyroptosis as the cause of reduced viability in cytokine
679 treated organoids. Pan-caspase inhibition (Z-VAD-FMK) also did not rescue viability,



Downloaded from journals.physiology.org/journal/ajpgi at Univ Col Cork (143.239.045.011) on October 3, 2022.

680 suggesting apoptosis alone was not responsible. Using live microscopy in combination with
681 the necrosis dye SYTOX Green, we determined that the loss of viability in cytokine treated
682 organoids was due to cell death (Fig. 8e). Cytokine treated organoids displayed multiple
683 SYTOX Green positive cells and disruption of epithelial barrier integrity. Tofacitinib treatment
684 reduced SYTOX green signal and prevented complete disruption of organoid integrity.

685 To test for tofacitinib activity we measured the production of CXCL10, a Th1
686 chemokine known to be induced by IFN-γ. Cytokine co-treatments increased secretion of
687 CXCL10 (Fig. S6c), which was significantly reduced by tofacitinib but unaffected by the other
688 inhibitors. Tofacitinib blocked the increased release of IL-1β/IL-18 in organoids treated with
689 IFN-β or IFN-γ in combination with TNF-α (Fig. 8d). None of the other inhibitors significantly
690 reduced IL-1β/IL-18 release (Fig. 8d), excluding the involvement of the NLRP3 and PYHIN
691 family inflammasomes. Unexpectedly, IL-18 release induced by cytokine co-treatment was
692 significantly increased by caspase inhibition (Fig. 8d). In summary, both cell death and IL-
693 1β/IL-18 release in organoids treated with IFN-β or IFN-γ in combination with TNF-α are
694 dependent on JAK kinase activity and independent of NLRP3 and caspase enzymatic
695 activity.
696



Downloaded from journals.physiology.org/journal/ajpgi at Univ Col Cork (143.239.045.011) on October 3, 2022.

## Discussion

We report that patients with active UC have increased colonic gene expression of several cytosolic DNA sensors – *AIM2*, *IFI16*, *ZBP1*, *cGAS* and *DHX9*, as well as the putative DNA sensors – *MNDA*, *PYHIN1* and *DDX41*. We show that inflammasome, STING and type I IFN signalling pathway genes downstream of these DNA sensor pathways are also elevated and active in patients with UC. Analysis of a UC single cell dataset showed that DNA sensor expression is cell type specific and increased in multiple immune and epithelial cell lineages from patients with active and inactive disease. This cell type specific expression pattern of DNA sensor pathway genes in UC was recapitulated in primary colonic epithelial organoids and macrophages treated with cytokines. We also report that while inhibition of canonical NLRP3 and inflammasome activity in whole biopsy tissue from patients with active UC reduced production of IL-1β this was not the case in primary colonic epithelial organoids. Finally, we show that treatment of colonic epithelial cells with type I or type II IFNs in combination with TNF-α induced JAK-dependent but inflammasome-independent production of IL-1β and inflammatory cell death. Collectively this biology may contribute to the developing picture of UC pathogenesis and mechanistically its inhibition may underpin the efficacy of JAK inhibitors in UC.

UC is thought to be triggered by environmental factors which perturb the epithelial barrier, alter the gut microbiota and stimulate mucosal immune inflammatory responses at the cellular interface between the epithelium and the LP. Recent advances (2) have contributed further to this framework by identifying (i) UC-specific susceptibility genes implicating epithelial dysfunction, (ii) loss of mitochondrial homeostasis in the epithelium leading to defective energy production, increased oxidative stress, and the release of inflammatory damage-associated molecular patterns (DAMPs) such as mitochondrial DNA, (iii) an impaired epithelial barrier as a pathogenic factor for UC, (iv) an epithelial transcriptional profile in inflamed UC mucosa characterised by enrichment for IFN-γ signalling pathways, (v) neutrophil accumulation, extra-cellular traps and neutrophil



Downloaded from journals.physiology.org/journal/ajpgi at Univ Col Cork (143.239.045.011) on October 3, 2022.

724 inflammatory cell death as drivers of inflammation, (vi) IL-1-driven stromal-neutrophil
725 interactions and cytokine networks responsible for monocyte IL-23 production, pathogenic T-
726 cell responses and resistance to therapies such as anti-TNFs (51, 52), (vii) a highly
727 dysregulated B cell response (53) and (viii) new epithelial, stromal, monocyte and T-cell
728 subsets and their interaction hubs from single cell datasets (2). Collectively, these recent
729 advances align with well-known clinical features of UC including a serological marker profile
730 characterised by anti p-neutrophil cytoplasmic antibodies (pANCA), anti-dsDNA, anti-IFI16
731 and anti-goblet cell antibodies and histopathology marked by distorted crypt architecture,
732 goblet cell depletion, neutrophil accumulation at crypt abscesses and submucosal fibrosis
733 (2). Our data showing that DNA sensor associated type I Interferon signalling is increased in
734 UC aligns with these molecular, pathogenic and clinical features of the disease and suggests
735 that the source of dsDNA as stimulus for these DNA sensor pathways could be host in
736 origin. Potential sources of this host DNA include mitochondrial DNA from the epithelium
737 associated with the suggested mitochondriopathy in UC (54) and/or DNA from dying
738 neutrophils and epithelial cells.

739 IL-1β has recently emerged as a critical pro-inflammatory cytokine and therapeutic
740 target in IBD, particularly in those patients that are resistant to therapies, have deep
741 ulceration, with neutrophil accumulation, epithelial cell damage in ulcers, and that express
742 high levels of *IL1B* (6, 51, 52, 55). The inflammasome is required for maturation of IL-1β and
743 can be activated by PYHIN family members AIM2 and IFI16 upon their sensing of DNA. We
744 confirmed and expanded on previous studies which showed an increased expression of
745 IFI16 and AIM2 in colonic tissue of patients with active UC (49). Interestingly, our analysis of
746 a UC single cell dataset and *in vitro* experiments with primary human macrophages and
747 colonic epithelial organoids revealed a cell-type specific expression pattern for AIM2 and
748 IFI16 and other PYHIN family members with little to no AIM2 expression detectable in
749 epithelial cells. One interpretation of this data is that AIM2 expression may be silenced in
750 epithelial cells to protect them from activation of the AIM2 inflammasome and pyroptosis in
751 response to microbial and host DNA. MCC950 is a highly selective small molecule inhibitor



Downloaded from journals.physiology.org/journal/ajpgi at Univ Col Cork (143.239.045.011) on October 3, 2022.

752 of both the canonical and non-canonical NLRP3 inflammasome and does not inhibit DNA
753 sensing inflammasomes (56). Using an *ex vivo* colonic mucosal biopsy system and MCC950
754 we confirmed that release of IL-1β is increased in active UC and partially dependent on
755 NLRP3. IL-1β release was further decreased in this *ex vivo* system using the Caspase-1
756 inhibitor VX-765. This suggests that Caspase-1 dependent inflammasomes other than
757 NLRP3, such as the PYHIN family sensors, could be contributing towards IL-1β production
758 in active UC tissue. We also discovered that colonic epithelial organoids secrete IL-1β while
759 executing IFN and TNF-α induced cell death. Although the concentration of IL-1β detected
760 was relatively low, it has been demonstrated that even in the low pg/mL range IL-1β can
761 induce ER stress and metabolic dysfunction in primary cells (67). During pyroptosis the
762 release of IL-1β from cells is facilitated by caspase-1 cleaved Gasdermin D, which creates
763 pores in the plasma membrane. Surprisingly, we found that the secretion of IL-1β by
764 organoids was independent of the canonical caspase-1 inflammasome. While there is
765 substantial evidence for non-canonical processing of pro-IL-1β by caspase-8 in innate
766 immune cells (71) inhibition of capase-8 also did not prevent IL-1β release from organoids.
767 Pro-IL-1β can be processed independently of caspases by proteases including elastase,
768 cathepsin G and chymase excreted from neutrophils and mast cells (71). As already
769 discussed, during active UC there is extensive infiltration of the colonic LP by activated
770 neutrophils, which could provide a source of proteases for the processing of pro-IL-1β
771 released by the colonic epithelium. Overall, our data indicate that IL-1β release in actively
772 inflamed UC tissue is partially NLRP3-dependent but substantially caspase-1
773 inflammasome-dependent with the potential for NLRP3 and caspase-independent release
774 from dying epithelial cells.

775 We found that patients with active UC are fully competent for activation of the type I
776 IFN response and have an increased expression of direct type I IFN responsive target
777 genes. An increase in type I IFN-stimulated genes in UC colonic tissue has previously been
778 reported (14) and two studies have described how an increased type I IFN signature in
779 peripheral blood and colonic biopsies of patients with IBD is associated with non-response to



Downloaded from journals.physiology.org/journal/ajpgi at Univ Col Cork (143.239.045.011) on October 3, 2022.

780 anti-TNF-α biologics (15, 43). However, the role of type I IFN role in intestinal inflammation is
781 controversial. During infection, type I IFN regulated ISGs have potent antimicrobial activities
782 and can induce the production of inflammatory cytokines and activate the inflammasome
783 (57, 58). However, they also work concurrently to resolve infection and inflammation by
784 promoting epithelial restitution, maturation of dendritic cells and Treg differentiation (57, 58).
785 Due to these anti-inflammatory characteristics; type I IFNs have been investigated as
786 treatment options for IBD and other immune disorders. However, results from UC clinical
787 trials in patients with active disease have been inconclusive, with a small increase in
788 remission rates observed when compared to placebo, but this did not reach significance
789 (59). Additionally, case studies reported hepatitis C and multiple sclerosis patients
790 developing or experiencing exacerbated existing UC while receiving type I IFN therapy (60,
791 61).

792 The transcriptional signature we found in colonic mucosal biopsy tissue from patients
793 with active UC was partially mimicked in non-IBD human colonic organoids treated with IFN-
794 β alone or in combination with TNF-α. Importantly, using IHC we determined that ZBP1 and
795 IFI16 are expressed preferentially in the epithelium of colonic tissue from patients with UC;
796 and are increased during inflammation. This further supports our interpretation that the
797 transcriptional profile in IFN-β treated colonic epithelial organoids is likely tissue and disease
798 relevant. Induction of *IFI16*, *ZBP1* and *cGAS* gene expression by IFN treatment in other
799 systems has been previously reported (47, 62-64). Co-regulation and positive feedback
800 regulation between type I IFN and cGAS/ZBP1-STING signalling has also been
801 demonstrated, with both cGAS and ZBP1 requiring IFNAR1 to mount a full response against
802 cytosolic DNA (22, 47). Overall, this DNA sensor and type I IFN gene expression signature is
803 similar to that found in type I interferonopathies (6, 55) and may be reflective of the overall
804 immunopathogenesis in UC which is associated with disruption of epithelial barrier integrity,
805 increased inflammatory cell death, release of DAMPs such as mitochondrial and nuclear
806 dsDNA and an auto-immune-like serological profile (2).



Downloaded from journals.physiology.org/journal/ajpgi at Univ Col Cork (143.239.045.011) on October 3, 2022.

In addition to increasing the expression of DNA sensor pathway genes, we found that treatment of colonic epithelial organoids with IFN-β or IFN-γ in combination with TNF-α induced inflammatory cell death. Recent single cell RNA-Seq studies have revealed that epithelial cells in the inflamed UC mucosa showed upregulation of several inflammatory pathways (33, 65), notably IFN-γ signalling, and there are several recent reports highlighting the cytotoxic effect of IFNs alone or in combination with TNF-α on the intestinal epithelium (29, 66-68). Increased colonic epithelial cell death has also been reported in chronic UC, and administration of anti-TNF-α biologics reduces cell death levels (69). While previous studies in cytokine-treated murine intestinal organoid cultures have suggested that cell death was caspase-dependent we found that cell death of human colonic organoids induced by IFN-β or IFN-γ in combination with TNF-α was independent of caspase activity. In terms of identifying mechanisms for this type of inflammatory cell death we and others have investigated other modes of caspase independent cell death such as necroptosis. Expression of the necroptotic regulator RIPK3 is associated with disease severity in UC (70), and IFNs can induce ZBP1 regulated necroptotic cell death (21, 22). Previously, our lab has reported that combined inhibition of necroptotic executors RIPK1, RIPK3 and MLKL in undifferentiated colonic organoids and perturbation of ZBP1 in HT29 cells could not rescue cell death induced by IFN-γ in combination with TNF-α (29). Therefore, the cell death observed in colonic organoid cultures in this study is unlikely to be classical necroptosis or PANoptosis.

Treatment with the JAK1/3 inhibitor tofacitinib inhibited both IL-1β/IL-18 release and cell death induced by IFN-β or IFN-γ in combination with TNF-α, which indicates the JAK/STAT-dependent nature of this cell death pathway. There is evidence to suggest that JAK/STAT signalling driven by type I IFN has a role in IBD pathology and anti-TNF-α resistance, which may explain why tofacitinib is an effective therapy for patients with UC who are refractive to anti-TNF-α biologics (71). IBD patients who do not respond to infliximab have an elevated type I IFN signature that is sustained after treatment (15, 43). Conversely, responders have a lower baseline signature that reduces significantly post-treatment. In a



Downloaded from journals.physiology.org/journal/ajpgi at Univ Col Cork (143.239.045.011) on October 3, 2022.

murine DSS model IFN-β reduced inflammation during the acute phase of inflammation but prolonged disease during recovery (72). Notably, during recovery IFN-β increased levels of colonic epithelial cell death. This conflicts with the protective anti-apoptotic effects of type I IFN on the epithelium (57, 58). As there are 13 type I IFN genes in humans the contribution of type I IFNs to IBD could be subtype and context dependent and a deeper analysis of the cell type specific nature of type I IFN gene expression in UC is required. Perhaps the activities of type I IFN during intestinal inflammation depend on the subtype, the strength of the signal and interactions with other cytokine pathways such as TNF-α. It is possible that in patients who are refractory to anti-TNF-α the high levels of IFN-β that persist after treatment tip the balance from proliferation and healing to cell death and inflammation.

We propose that the increased activity of DNA sensor pathways and type I IFN signalling we observed in active UC is reflective of and contributes to the overall immunopathogenesis of this disease. This could occur through a positive feedback loop whereby host nuclear and mitochondrial DNA released from dying cells leads to sustained pathogenic IFN-β signalling and damage to the epithelium. The inflammatory cell death phenotype we discovered in IFN-β and TNF-α co-treated colonic organoids is relevant to UC immunopathology; and may help explain the efficacy of JAKinibs in this disease.

**Funding**

This work was supported by Science Foundation Ireland — namely a research centre grant (SFI-12/RC/2273) and a research centre spoke award (SFI-14/SP/2710) to APC Microbiome Ireland. In addition, part of this work was supported by separate research funding from Second Genome to APC Microbiome Ireland.

**Conflict of Interest**

The authors have no conflict of interest in relation to this study. K.N. and F.S. are in receipt of research funding from AbbVie Inc. as part of a research centre spoke award (SFI-



Downloaded from journals.physiology.org/journal/ajpgi at Univ Col Cork (143.239.045.011) on October 3, 2022.

14/SP/2710) to APC Microbiome Ireland and have received research funding in the past from Second Genome. B.L.M. was an employee and shareholder of AbbVie Inc. during the time the work was completed. K.D. is an employee of Second Genome, Inc. and holds stock options in Second Genome, Inc. and G.S.D was an employee of Second Genome Inc. during the time part of the work was completed.

**Author Contributions**

K.N. conceived, designed and directed the study. P.F., A.F., J.A.W, A.C., A.V., A.H., S.McS.,S.R., A.H., E.B., A.S., M.B., M.A., G.M., J.MacS., M-I.H., M.H., and C.F., designed and carried out experimental work. P.F. and J.A.W. performed and analysed all organoid-based experiments. T.C. performed bioinformatic analysis of open access single cell UC datasets. E.M.Q., F.S., S.A.Z., J.M. M.H., and C.F consented patients and coordinated collection of all mucosal biopsies; B.L.M. and S.M. advised on the design of JAK inhibitor experiments and G.S.D and K.D., advised on design of NLRP3 and Caspase inhibitor experiments in organoids and whole biopsies. P.F., A.F. and K.N wrote the manuscript and co-authors reviewed, edited and approved final version of the manuscript.

**Acknowledgements**

The authors would also like to thank the patients for their informed consent and participation in the research study, and the clinical personnel for their excellent assistance. Graphical abstract was partially created with BioRender.com.

**Materials and Data Availability**

Contact corresponding author for access to materials and data.



Downloaded from journals.physiology.org/journal/ajpgi at Univ Col Cork (143.239.045.011) on October 3, 2022.

## References


1. **Chang JT**. Pathophysiology of Inflammatory Bowel Diseases. *N Engl J Med* 383: 2652-2664, 2020.
2. **Porter RJ, Kalla R, and Ho GT**. Ulcerative colitis: Recent advances in the understanding of disease pathogenesis. *F1000Res* 9: 2020.
3. **Fukata M, and Arditi M**. The role of pattern recognition receptors in intestinal inflammation. *Mucosal Immunol* 6: 451-463, 2013.
4. **Walsh D, McCarthy J, O'Driscoll C, and Melgar S**. Pattern recognition receptors--molecular orchestrators of inflammation in inflammatory bowel disease. *Cytokine Growth Factor Rev* 24: 91-104, 2013.
5. **Abraham C, Abreu MT, and Turner JR**. Pattern Recognition Receptor Signaling and Cytokine Networks in Microbial Defenses and Regulation of Intestinal Barriers: Implications for Inflammatory Bowel Disease. *Gastroenterology* 162: 1602-1616 e1606, 2022.
6. **Uggenti C, Lepelley A, and Crow YJ**. Self-Awareness: Nucleic Acid-Driven Inflammation and the Type I Interferonopathies. *Annu Rev Immunol* 37: 247-267, 2019.
7. **Paludan SR, and Bowie AG**. Immune sensing of DNA. *Immunity* 38: 870-880, 2013.
8. **Elkon KB**. Review: Cell Death, Nucleic Acids, and Immunity: Inflammation Beyond the Grave. *Arthritis Rheumatol* 70: 805-816, 2018.
9. **Ansari MA, Singh VV, Dutta S, Veettil MV, Dutta D, Chikoti L, Lu J, Everly D, and Chandran B**. Constitutive interferon-inducible protein 16-inflammasome activation during Epstein-Barr virus latency I, II, and III in B and epithelial cells. *J Virol* 87: 8606-8623, 2013.
10. **Rathinam VA, Jiang Z, Waggoner SN, Sharma S, Cole LE, Waggoner L, Vanaja SK, Monks BG, Ganesan S, Latz E, Hornung V, Vogel SN, Szomolanyi-Tsuda E, and Fitzgerald KA**. The AIM2 inflammasome is essential for host defense against cytosolic bacteria and DNA viruses. *Nat Immunol* 11: 395-402, 2010.
11. **Boyapati RK, Dorward DA, Tamborska A, Kalla R, Ventham NT, Doherty MK, Whitfield PD, Gray M, Loane J, Rossi AG, Satsangi J, and Ho GT**. Mitochondrial DNA Is a Pro-Inflammatory Damage-Associated Molecular Pattern Released During Active IBD. *Inflamm Bowel Dis* 24: 2113-2122, 2018.
12. **Vrakas S, Mountzouris KC, Michalopoulos G, Karamanolis G, Papatheodoridis G, Tzathas C, and Gazouli M**. Intestinal Bacteria Composition and Translocation of Bacteria in Inflammatory Bowel Disease. *PLoS One* 12: e0170034, 2017.
13. **Gutierrez A, Zapater P, Juanola O, Sempere L, Garcia M, Laveda R, Martinez A, Scharl M, Gonzalez-Navajas JM, Such J, Wiest R, Rogler G, and Frances R**. Gut Bacterial DNA Translocation is an Independent Risk Factor of Flare at Short Term in Patients With Crohn's Disease. *Am J Gastroenterol* 111: 529-540, 2016.
14. **Ostvik AE, Svendsen TD, Granlund AVB, Doseth B, Skovdahl HK, Bakke I, Thorsvik S, Afroz W, Walaas GA, Mollnes TE, Gustafsson BI, Sandvik AK, and Bruland T**. Intestinal Epithelial Cells Express Immunomodulatory ISG15 During Active Ulcerative Colitis and Crohn's Disease. *J Crohns Colitis* 14: 920-934, 2020.
15. **Mavragani CP, Nezos A, Dovrolis N, Andreou NP, Legaki E, Sechi LA, Bamias G, and Gazouli M**. Type I and II Interferon Signatures Can Predict the Response to Anti-TNF Agents in Inflammatory Bowel Disease Patients: Involvement of the Microbiota. *Inflamm Bowel Dis* 26: 1543-1553, 2020.
16. **Bauer C, Duewell P, Mayer C, Lehr HA, Fitzgerald KA, Dauer M, Tschopp J, Endres S, Latz E, and Schnurr M**. Colitis induced in mice with dextran sulfate sodium (DSS) is mediated by the NLRP3 inflammasome. *Gut* 59: 1192-1199, 2010.
17. **Itani S, Watanabe T, Nadatani Y, Sugimura N, Shimada S, Takeda S, Otani K, Hosomi S, Nagami Y, Tanaka F, Kamata N, Yamagami H, Tanigawa T, Shiba M, Tominaga K, Fujiwara Y, and Arakawa T**. NLRP3 inflammasome has a protective effect against oxazolone-induced colitis: a possible role in ulcerative colitis. *Sci Rep* 6: 39075, 2016.




Downloaded from journals.physiology.org/journal/ajpgi at Univ Col Cork (143.239.045.011) on October 3, 2022.

18. **Zaki MH, Boyd KL, Vogel P, Kastan MB, Lamkanfi M, and Kanneganti TD**. The NLRP3 inflammasome protects against loss of epithelial integrity and mortality during experimental colitis. *Immunity* 32: 379-391, 2010.
19. **Ratsimandresey RA, Indramohan M, Dorfleutner A, and Stehlik C**. The AIM2 inflammasome is a central regulator of intestinal homeostasis through the IL-18/IL-22/STAT3 pathway. *Cell Mol Immunol* 14: 127-142, 2017.
20. **Nunes T, Bernardazzi C, and de Souza HS**. Cell death and inflammatory bowel diseases: apoptosis, necrosis, and autophagy in the intestinal epithelium. *Biomed Res Int* 2014: 218493, 2014.
21. **Yang D, Liang Y, Zhao S, Ding Y, Zhuang Q, Shi Q, Ai T, Wu SQ, and Han J**. ZBP1 mediates interferon-induced necroptosis. *Cell Mol Immunol* 17: 356-368, 2020.
22. **Chen D, Tong J, Yang L, Wei L, Stolz DB, Yu J, Zhang J, and Zhang L**. PUMA amplifies necroptosis signaling by activating cytosolic DNA sensors. *Proc Natl Acad Sci U S A* 115: 3930-3935, 2018.
23. **Malireddi RKS, Kesavardhana S, and Kanneganti TD**. ZBP1 and TAK1: Master Regulators of NLRP3 Inflammasome/Pyroptosis, Apoptosis, and Necroptosis (PAN-optosis). *Front Cell Infect Microbiol* 9: 406, 2019.
24. **Murthy AMV, Robinson N, and Kumar S**. Crosstalk between cGAS-STING signaling and cell death. *Cell Death Differ* 27: 2989-3003, 2020.
25. **Sato T, Stange DE, Ferrante M, Vries RG, Van Es JH, Van den Brink S, Van Houdt WJ, Pronk A, Van Gorp J, Siersema PD, and Clevers H**. Long-term expansion of epithelial organoids from human colon, adenoma, adenocarcinoma, and Barrett's epithelium. *Gastroenterology* 141: 1762-1772, 2011.
26. **VanDussen KL, Marinshaw JM, Shaikh N, Miyoshi H, Moon C, Tarr PI, Ciorba MA, and Stappenbeck TS**. Development of an enhanced human gastrointestinal epithelial culture system to facilitate patient-based assays. *Gut* 64: 911-920, 2015.
27. **Miyoshi H, and Stappenbeck TS**. In vitro expansion and genetic modification of gastrointestinal stem cells in spheroid culture. *Nat Protoc* 8: 2471-2482, 2013.
28. **Woznicki JA, Flood P, Bustamante-Garrido M, Stamou P, Moloney G, Fanning A, Zulquernain SA, McCarthy J, Shanahan F, Melgar S, and Nally K**. Human BCL-G regulates secretion of inflammatory chemokines but is dispensable for induction of apoptosis by IFN-gamma and TNF-alpha in intestinal epithelial cells. *Cell Death Dis* 11: 68, 2020.
29. **Woznicki JA, Saini N, Flood P, Rajaram S, Lee CM, Stamou P, Skowyra A, Bustamante-Garrido M, Regazzoni K, Crawford N, McDade SS, Longley DB, Aza-Blanc P, Shanahan F, Zulquernain SA, McCarthy J, Melgar S, McRae BL, and Nally K**. TNF-alpha synergises with IFN-gamma to induce caspase-8-JAK1/2-STAT1-dependent death of intestinal epithelial cells. *Cell Death Dis* 12: 864, 2021.
30. **Miyoshi H, and Stappenbeck TS**. In vitro expansion and genetic modification of gastrointestinal stem cells as organoids. *Nature protocols* 8: 2471-2482, 2013.
31. **Livak KJ, and Schmittgen TD**. Analysis of relative gene expression data using real-time quantitative PCR and the 2(-Delta Delta C(T)) Method. *Methods* 25: 402-408, 2001.
32. **Fahlgren A, HAMMARSTRÖM S, DANIELSSON Å, and HAMMARSTRÖM M-L**. Increased expression of antimicrobial peptides and lysozyme in colonic epithelial cells of patients with ulcerative colitis. *Clinical and Experimental Immunology* 131: 90–101, 2003.
33. **Smillie CS, Biton M, Ordovas-Montanes J, Sullivan KM, Burgin G, Graham DB, Herbst RH, Rogel N, Slyper M, Waldman J, Sud M, Andrews E, Velonias G, Haber AL, Jagadeesh K, Vickovic S, Yao J, Stevens C, Dionne D, Nguyen LT, Villani AC, Hofree M, Creasey EA, Huang H, Rozenblatt-Rosen O, Garber JJ, Khalili H, Desch AN, Daly MJ, Ananthakrishnan AN, Shalek AK, Xavier RJ, and Regev A**. Intra- and Inter-cellular Rewiring of the Human Colon during Ulcerative Colitis. *Cell* 178: 714-730 e722, 2019.
34. **Hao Y, Hao S, Andersen-Nissen E, Mauck WM, 3rd, Zheng S, Butler A, Lee MJ, Wilk AJ, Darby C, Zager M, Hoffman P, Stoeckius M, Papalexi E, Mimitou EP, Jain J, Srivastava A, Stuart T,**



Downloaded from journals.physiology.org/journal/ajpgi at Univ Col Cork (143.239.045.011) on October 3, 2022.

**Fleming LM, Yeung B, Rogers AJ, McElrath JM, Blish CA, Gottardo R, Smibert P, and Satija R**. Integrated analysis of multimodal single-cell data. *Cell* 184: 3573-3587 e3529, 2021.

35. **Wickham H**. *ggplot2: Elegant Graphics for Data Analysis*. Springer-Verlag New York, 2016.

36. **Garnier S, Ross N, Rudis R, Camargo PA, Sciaini M, and Scherer C**. Viridis - Colorblind-Friendly Color Maps for R. https://zenodo.org/record/4679424#.YwOwHBzMK3A, 2021.

37. **Sturn A, Quackenbush J, and Trajanoski Z**. Genesis: cluster analysis of microarray data. *Bioinformatics* 18: 207-208, 2002.

38. **Abe T, Lee A, Sitharam R, Kesner J, Rabadan R, and Shapira SD**. Germ-Cell-Specific Inflammasome Component NLRP14 Negatively Regulates Cytosolic Nucleic Acid Sensing to Promote Fertilization. *Immunity* 46: 621-634, 2017.

39. **Greuter T, Manser C, Pittet V, Vavricka SR, Biedermann L, and on behalf of Swiss Ibdnet aowgotSSoG**. Gender Differences in Inflammatory Bowel Disease. *Digestion* 101 Suppl 1: 98-104, 2020.

40. **Carter MJ, Jones S, Camp NJ, Cox A, Mee J, Warren B, Duff GW, Lobo AJ, and di Giovine FS**. Functional correlates of the interleukin-1 receptor antagonist gene polymorphism in the colonic mucosa in ulcerative colitis. *Genes Immun* 5: 8-15, 2004.

41. **Primiano MJ, Lefker BA, Bowman MR, Bree AG, Hubeau C, Bonin PD, Mangan M, Dower K, Monks BG, Cushing L, Wang S, Guzova J, Jiao A, Lin LL, Latz E, Hepworth D, and Hall JP**. Efficacy and Pharmacology of the NLRP3 Inflammasome Inhibitor CP-456,773 (CRID3) in Murine Models of Dermal and Pulmonary Inflammation. *J Immunol* 197: 2421-2433, 2016.

42. **Gu L, Casserly D, Brady G, Carpenter S, Bracken AP, Fitzgerald KA, Unterholzner L, and Bowie AG**. Myeloid cell nuclear differentiation antigen controls the pathogen-stimulated type I interferon cascade in human monocytes by transcriptional regulation of IRF7. *Nat Commun* 13: 14, 2022.

43. **Samie M, Lim J, Verschueren E, Baughman JM, Peng I, Wong A, Kwon Y, Senbabaoglu Y, Hackney JA, Keir M, McKenzie B, Kirkpatrick DS, van Lookeren Campagne M, and Murthy A**. Selective autophagy of the adaptor TRIF regulates innate inflammatory signaling. *Nat Immunol* 19: 246-254, 2018.

44. **Sims P, Coffman RL, and Hessel EM**. Biomarkers measuring the activity of Toll-like receptor ligands in clinical development programs. *Methods Mol Biol* 517: 415-440, 2009.

45. **Jones JW, Kayagaki N, Broz P, Henry T, Newton K, O'Rourke K, Chan S, Dong J, Qu Y, Roose-Girma M, Dixit VM, and Monack DM**. Absent in melanoma 2 is required for innate immune recognition of Francisella tularensis. *Proc Natl Acad Sci U S A* 107: 9771-9776, 2010.

46. **Harrison OJ, Srinivasan N, Pott J, Schiering C, Krausgruber T, Ilott NE, and Maloy KJ**. Epithelial-derived IL-18 regulates Th17 cell differentiation and Foxp3(+) Treg cell function in the intestine. *Mucosal Immunol* 8: 1226-1236, 2015.

47. **Ma F, Li B, Liu SY, Iyer SS, Yu Y, Wu A, and Cheng G**. Positive feedback regulation of type I IFN production by the IFN-inducible DNA sensor cGAS. *J Immunol* 194: 1545-1554, 2015.

48. **Schulzke JD, Bojarski C, Zeissig S, Heller F, Gitter AH, and Fromm M**. Disrupted barrier function through epithelial cell apoptosis. *Ann N Y Acad Sci* 1072: 288-299, 2006.

49. **Schaupp L, Muth S, Rogell L, Kofoed-Branzk M, Melchior F, Lienenklaus S, Ganal-Vonarburg SC, Klein M, Guendel F, Hain T, Schutze K, Grundmann U, Schmitt V, Dorsch M, Spanier J, Larsen PK, Schwanz T, Jackel S, Reinhardt C, Bopp T, Danckwardt S, Mahnke K, Heinz GA, Mashreghi MF, Durek P, Kalinke U, Kretz O, Huber TB, Weiss S, Wilhelm C, Macpherson AJ, Schild H, Diefenbach A, and Probst HC**. Microbiota-Induced Type I Interferons Instruct a Poised Basal State of Dendritic Cells. *Cell* 181: 1080-1096 e1019, 2020.

50. **Krishnaswami S, Wang T, Yuan Y, Alvey CW, Checchio T, Peterson M, Shi H, and Riese R**. Single- and multiple-dose pharmacokinetics of tofacitinib in healthy Chinese volunteers. *Clin Pharmacol Drug Dev* 4: 395-399, 2015.

51. **Aschenbrenner D, Quaranta M, Banerjee S, Ilott N, Jansen J, Steere B, Chen Y-H, Ho S, Cox K, Arancibia-Cárcamo CV, Coles M, Gaffney E, Travis SP, Denson L, Kugathasan S, Schmitz J, Powrie**



Downloaded from journals.physiology.org/journal/ajpgi at Univ Col Cork (143.239.045.011) on October 3, 2022.

**F, Sansom SN, and Uhlig HH**. Deconvolution of monocyte responses in inflammatory bowel disease reveals an IL-1 cytokine network that regulates IL-23 in genetic and acquired IL-10 resistance. *Gut* 70: 1023-1036, 2021.

52. **Friedrich M, Pohin M, Jackson MA, Korsunsky I, Bullers SJ, Rue-Albrecht K, Christoforidou Z, Sathananthan D, Thomas T, Ravindran R, Tandon R, Peres RS, Sharpe H, Wei K, Watts GFM, Mann EH, Geremia A, Attar M, Oxford IBDCI, Roche Fibroblast Network C, McCuaig S, Thomas L, Collantes E, Uhlig HH, Sansom SN, Easton A, Raychaudhuri S, Travis SP, and Powrie FM**. IL-1-driven stromal-neutrophil interactions define a subset of patients with inflammatory bowel disease that does not respond to therapies. *Nat Med* 27: 1970-1981, 2021.

53. **Uzzan M, Martin JC, Mesin L, Livanos AE, Castro-Dopico T, Huang R, Petralia F, Magri G, Kumar S, Zhao Q, Rosenstein AK, Tokuyama M, Sharma K, Ungaro R, Kosoy R, Jha D, Fischer J, Singh H, Keir ME, Ramamoorthi N, Gorman WEO, Cohen BL, Rahman A, Cossarini F, Seki A, Leyre L, Vaquero ST, Gurunathan S, Grasset EK, Losic B, Dubinsky M, Greenstein AJ, Gottlieb Z, Legnani P, George J, Irizar H, Stojmirovic A, Brodmerkel C, Kasarkis A, Sands BE, Furtado G, Lira SA, Tuong ZK, Ko HM, Cerutti A, Elson CO, Clatworthy MR, Merad M, Suarez-Farinas M, Argmann C, Hackney JA, Victora GD, Randolph GJ, Kenigsberg E, Colombel JF, and Mehandru S**. Ulcerative colitis is characterized by a plasmablast-skewed humoral response associated with disease activity. *Nat Med* 28: 766-779, 2022.

54. **Haberman Y, Karns R, Dexheimer PJ, Schirmer M, Somekh J, Jurickova I, Braun T, Novak E, Bauman L, Collins MH, Mo A, Rosen MJ, Bonkowski E, Gotman N, Marquis A, Nistel M, Rufo PA, Baker SS, Sauer CG, Markowitz J, Pfefferkorn MD, Rosh JR, Boyle BM, Mack DR, Baldassano RN, Shah S, Leleiko NS, Heyman MB, Griffiths AM, Patel AS, Noe JD, Aronow BJ, Kugathasan S, Walters TD, Gibson G, Thomas SD, Mollen K, Shen-Orr S, Huttenhower C, Xavier RJ, Hyams JS, and Denson LA**. Ulcerative colitis mucosal transcriptomes reveal mitochondriopathy and personalized mechanisms underlying disease severity and treatment response. *Nat Commun* 10: 38, 2019.

55. **Crow YJ, and Stetson DB**. The type I interferonopathies: 10 years on. *Nat Rev Immunol* 22: 471-483, 2022.

56. **Coll RC, Robertson AA, Chae JJ, Higgins SC, Munoz-Planillo R, Inserra MC, Vetter I, Dungan LS, Monks BG, Stutz A, Croker DE, Butler MS, Haneklaus M, Sutton CE, Nunez G, Latz E, Kastner DL, Mills KH, Masters SL, Schroder K, Cooper MA, and O'Neill LA**. A small-molecule inhibitor of the NLRP3 inflammasome for the treatment of inflammatory diseases. *Nat Med* 21: 248-255, 2015.

57. **Cho H, and Kelsall BL**. The role of type I interferons in intestinal infection, homeostasis, and inflammation. *Immunol Rev* 260: 145-167, 2014.

58. **Kotredes KP, Thomas B, and Gamero AM**. The Protective Role of Type I Interferons in the Gastrointestinal Tract. *Front Immunol* 8: 410, 2017.

59. **Pena-Rossi C, Schreiber S, Golubovic G, Mertz-Nielsen A, Panes J, Rachmilewitz D, Shieh MJ, Simanenkov VI, Stanton D, and Graffner H**. Clinical trial: a multicentre, randomized, double-blind, placebo-controlled, dose-finding, phase II study of subcutaneous interferon-beta-la in moderately active ulcerative colitis. *Aliment Pharmacol Ther* 28: 758-767, 2008.

60. **MITORO A, YOSHIKAWA M, YAMAMOTO K, MIMURA M, YOSHIKAWA Y, SHIROI A, MOCHI T, SAKAMOTO T, YAMAO J, KIKUCHI E, FUKUI H, and TSUJII T**. Exacerbation of ulcerative colitis during alpha-interferon therapy for chronic hepatitis C. *Internal Medicine* 32: 327-331, 1993.

61. **Tuna Y, Basar O, Dikici H, and Koklu S**. Rapid onset of ulcerative colitis after treatment with interferon beta1a in a patient with multiple sclerosis. *J Crohns Colitis* 5: 75-76, 2011.

62. **Wang Y, Hao Q, Florence JM, Jung BG, Kurdowska AK, Samten B, Idell S, and Tang H**. Influenza Virus Infection Induces ZBP1 Expression and Necroptosis in Mouse Lungs. *Front Cell Infect Microbiol* 9: 286, 2019.

63. **Fu Y, Comella N, Tognazzi K, Brown LF, Dvorak HF, and Kocher O**. Cloning of DLM-1, a novel gene that is up-regulated in activated macrophages, using RNA differential display. *Gene* 240: 157-163, 1999.



Downloaded from journals.physiology.org/journal/ajpgi at Univ Col Cork (143.239.045.011) on October 3, 2022.

64. **Veeranki S, Duan X, Panchanathan R, Liu H, and Choubey D**. IFI16 protein mediates the anti-inflammatory actions of the type-I interferons through suppression of activation of caspase-1 by inflammasomes. *PLoS One* 6: e27040, 2011.
65. **Parikh K, Antanaviciute A, Fawkner-Corbett D, Jagielowicz M, Aulicino A, Lagerholm C, Davis S, Kinchen J, Chen HH, Alham NK, Ashley N, Johnson E, Hublitz P, Bao L, Lukomska J, Andev RS, Bjorklund E, Kessler BM, Fischer R, Goldin R, Koohy H, and Simmons A**. Colonic epithelial cell diversity in health and inflammatory bowel disease. *Nature* 567: 49-55, 2019.
66. **Gunther C, Ruder B, Stolzer I, Dorner H, He GW, Chiriac MT, Aden K, Strigli A, Bittel M, Zeissig S, Rosenstiel P, Atreya R, Neurath MF, Wirtz S, and Becker C**. Interferon Lambda Promotes Paneth Cell Death Via STAT1 Signaling in Mice and Is Increased in Inflamed Ileal Tissues of Patients With Crohn's Disease. *Gastroenterology* 157: 1310-1322 e1313, 2019.
67. **Xu P, Becker H, Elizalde M, Pierik M, Masclee A, and Jonkers D**. Interleukin-28A induces epithelial barrier dysfunction in CD patient-derived intestinal organoids. *Am J Physiol Gastrointest Liver Physiol* 320: G689-G699, 2021.
68. **Constant DA, Van Winkle JA, VanderHoek E, Dekker SE, Sofia MA, Regner E, Modiano N, Tsikitis VL, and Nice TJ**. Transcriptional and Cytotoxic Responses of Human Intestinal Organoids to IFN Types I, II, and III. *Immunohorizons* 6: 416-429, 2022.
69. **Goretsky T, Dirisina R, Sinh P, Mittal N, Managlia E, Williams DB, Posca D, Ryu H, Katzman RB, and Barrett TA**. p53 mediates TNF-induced epithelial cell apoptosis in IBD. *Am J Pathol* 181: 1306-1315, 2012.
70. **Duan C, Xu X, Lu X, Wang L, and Lu Z**. RIP3 knockdown inhibits necroptosis of human intestinal epithelial cells via TLR4/MyD88/NF-kappaB signaling and ameliorates murine colitis. *BMC Gastroenterol* 22: 137, 2022.
71. **Biemans VBC, Sleutjes JAM, de Vries AC, Bodelier AGL, Dijkstra G, Oldenburg B, Lowenberg M, van Bodegraven AA, van der Meulen-de Jong AE, de Boer NKH, Srivastava N, West RL, Romkens TEH, Horjus Talabur Horje CS, Jansen JM, van der Woude CJ, Hoekstra J, Weersma RK, van Schaik FDM, Hoentjen F, Pierik MJ, Dutch Initiative on C, and Colitis**. Tofacitinib for ulcerative colitis: results of the prospective Dutch Initiative on Crohn and Colitis (ICC) registry. *Aliment Pharmacol Ther* 51: 880-888, 2020.
72. **Rauch I, Hainzl E, Rosebrock F, Heider S, Schwab C, Berry D, Stoiber D, Wagner M, Schleper C, Loy A, Urich T, Muller M, Strobl B, Kenner L, and Decker T**. Type I interferons have opposing effects during the emergence and recovery phases of colitis. *Eur J Immunol* 44: 2749-2760, 2014.



Downloaded from journals.physiology.org/journal/ajpgi at Univ Col Cork (143.239.045.011) on October 3, 2022.

**Figure 1. Screen of pattern recognition receptor expression in IBD colonic mucosal tissue reveals upregulation of DNA sensor pathway genes in active UC**

(a) Expression as measured by RT-qPCR of 42 PRR genes in active and inactive ulcerative colitis (UC) and Crohn's disease (CD) mucosal biopsies compared to non-IBD controls. The relative expression is displayed as a hierarchically clustered heatmap, red indicates up-regulation, blue represents down-regulation, black represents no change relative to the calibrator control and grey represents no detectable expression. (b) Scatter plots of *CIITA*, *NLRP1*, *NLRP14*, *TLR9*, *AIM2* and *ZBP1* (heatmap genes highlighted in green). Non-IBD control n=8 (male 5, female 3), active UC n=11 (male 7, female 4), inactive UC n=9 (male 4, female 5), active CD n=8 (male 1, female 7) and inactive CD n=8 (male 3, female 5) mucosal biopsies. Data are expressed as means ± SEM (standard error of the mean); one-way ANOVA analysis was performed followed by Dunnett's post-test # $p<0.05$, ## $p<0.01$, ### $p<0.001$ versus control group, or Tukey's multiple comparisons post-test * $p<0.05$, ** $p<0.01$, *** $p<0.001$ as indicated.

**Figure 2. PYHIN family DNA sensors and canonical inflammasome pathway genes are increased in active UC**

(a) Schematic of the PYHIN family DNA sensor and classic inflammasome pathways. (b) Relative expression of *AIM2*, *IFI16*, *PYHIN1* and *MNDA* in non-IBD control, UC active and UC inactive mucosal biopsies as measured by RT-qPCR. (c) Representative IFI16 staining of recto-sigmoid tissue (10 μm thick sections). Unstained non-IBD control (i) and stained non-IBD control (ii), inactive UC (iii & iv) and active UC (v & vi). White arrows indicating specific staining in stroma. Black arrowhead (iv & v) indicating specific staining in cells adjacent to the epithelium. White arrowheads indicate epithelial expression (vi). Scale bar – 100 μm. Images representative of n=4 non-IBD control (2 male and 2 female), n=3 UC active (2 male and 1 female) and n=4 UC inactive (1 male and 3 female) samples (d) Relative expression of the inflammasome caspase - *CASP1*, and caspase-1 regulated cytokines *IL1B*, *IL18* and *IL33* in control, UC inactive and UC active mucosal biopsies as measured by RT-qPCR. Non-IBD control n=31 (15 male, 16 female), UC active n=33 (17 male, 16 female) and UC inactive n=31 (15 male, 16 female) mucosal biopsies. (e) Protein concentration of IL-1β and IL-1RA detected in supernatant of overnight biopsy explant cultures treated with the inflammasome inhibitors - caspase-1 VX765 (50 μM) and NLRP3 MCC950 (10 μM), and ratio of IL-1RA/IL-1β measured. n=11 patients with active UC. Data are expressed as means ± SEM; (b, d) Kruskal-Wallis analysis followed by Dunn's post-test # $p<0.05$, ## $p<0.01$, ### $p<0.001$ versus control group, or * $p<0.05$, ** $p<0.01$, *** $p<0.001$ as indicated. (e) one-way ANOVA analysis was performed followed by Dunnett's post-test #



Downloaded from journals.physiology.org/journal/ajpgi at Univ Col Cork (143.239.045.011) on October 3, 2022.

p<0.05, ## p<0.01, ### p<0.001 versus control group, or Tukey's multiple comparisons post-test * p<0.05, ** p<0.01, *** p<0.001 as indicated.

**Figure 3: Expression of *IFI16* is increased in multiple colonic epithelial and immune cell lineages in active UC**

Analysis of open access UC single cell RNA-Seq dataset from Smillie *et al*., consisting of single cell preparations from colonic mucosal biopsies, n=12 healthy, n=18 active UC, n=18 Inactive UC (33). (a) t-SNE plot of epithelial cell populations from healthy, active UC and inactive UC samples combined. Coloured by cell subset assigned in cohort. (b) t-SNE plot of immune cell populations from healthy, active UC and inactive UC samples combined. Coloured by cell subset assigned in cohort. (c) t-SNE plots of epithelial cell populations from healthy, active UC and inactive UC samples showing relative expression of *AIM2*, *IFI16* (arrowhead, active UC $IFI16^{+}$ enterocyte cluster) and *CASP1* (arrowhead, active UC CASP1+ enterocyte cluster). (d) t-SNE plots of immune cell populations from healthy, active UC and inactive UC samples showing relative expression of *AIM2* (arrowhead, cycling B and T cells in active UC), *IFI16* (arrowheads, inflammatory monocytes in active/inactive UC) and *CASP1* (arrowheads, inflammatory monocytes in active/inactive UC). t-SNE plots from (a) and (b) are adapted from: https://singlecell.broadinstitute.org/single_cell.

**Figure 4: DNA sensors, *STING* and type I IFN signalling are upregulated in active UC**

(a) Schematic of DNA sensor pathways which induce type I Interferon (IFN). (b) *ZBP1* and *cGAS* expression measured by RT-qPCR in non-IBD control, UC inactive and UC active mucosal biopsies. (c) Representative ZBP1 staining of recto-sigmoid tissue (10 μm thick). Unstained non-IBD control (i) and stained non-IBD control (ii), inactive UC (iii & iv) and active UC (v & vi). White arrows indicate specific positive staining in stroma (ii, iii & iv). Black arrowheads indicate specific staining in cells adjacent to the epithelium (iv & v). White arrowheads indicate epithelial staining (vi). Scale bar – 100 μm. Images representative of n=3 non-IBD control (2 male and 1 female), n=4 UC active (3 male and 1 female) and n=3 UC inactive (1 male and 2 female) samples (d-g). Relative expression of downstream pathway components (d) *STING* and *TBK1*, (e) transcriptional regulators of Type I IFNs *IRF3* and *IRF7*, (f) type I IFN expression (*IFNA1* and *IFNB*) and (g) type I IFN responsive genes, *OAS2*, *IFIT2*, *MX1* and *MX2* as measured by RT-qPCR. Colonic mucosal biopsies from non-IBD control n=31 (15 male, 16 female), UC active n=33 (17 male,16 female) and UC inactive n=31 (15 male,16 female). Data are expressed as means ± SEM; (b, d, e, g) Kruskal-Wallis analysis followed by Dunn's post-test; # p<0.05, ## p<0.01, ### p<0.001 versus control



Downloaded from journals.physiology.org/journal/ajpgi at Univ Col Cork (143.239.045.011) on October 3, 2022.

group, or * p<0.05, ** p<0.01, *** p<0.001 as indicated. (f) Two-tailed Mann-Whitney test; * p<0.05, *** p<0.001 as indicated.

**Figure 5: *STING* expression is increased in multiple epithelial cell lineages in active and inactive UC**

Analysis of open access UC single cell RNA-seq dataset from Smillie *et al*., consisting of single cell preparations from colonic mucosal biopsies, n=12 healthy, n=18 active UC, n=18 Inactive UC (33). (a) t-SNE plot of epithelial cell populations from healthy, active UC and inactive UC samples combined. Coloured by cell subset assigned in cohort. (b) t-SNE plot of immune cell populations from healthy, active UC and inactive UC samples combined. Coloured by cell subset assigned in cohort. (c) t-SNE plots of epithelial cell populations from healthy, active UC and inactive UC samples showing relative expression of *ZBP1* (arrowhead, active UC *ZBP1*+ enterocyte cluster), *cGAS* and *STING* (arrowheads, M cell clusters in active/inactive UC). (d) t-SNE plots of immune cell populations from healthy, active UC and inactive UC samples showing relative expression of *ZBP1* (arrowheads, cycling B and T cells in active/inactive UC, arrows, plasma cells in active/inactive UC), *cGAS* (arrowheads, cycling B and T cells in active/inactive UC, arrow, inflammatory monocytes in active UC) and *STING* (arrowheads, inflammatory monocytes in active/inactive UC, arrows, Tregs in active/inactive UC). t-SNE plots from (a) and (b) are adapted from: https://singlecell.broadinstitute.org/single_cell.

**Figure 6: Type I and II IFN treatment increases IFI16 and inflammasome pathway gene expression in human colonic organoids**

(a) Live phase contrast microscopy (4x objective lens, 40x inset images), representative images of n=2 non-IBD lines of undifferentiated human colonic organoids treated as follows; 1) Ctrl (untreated), 2) IFN-γ - 10 ng/mL, 3) IFN-β - 25 ng/mL 4) TNF-α - 10 ng/mL, 5) IFN-γ + TNF-α (10 ng/mL + 10 ng/mL), and 6) IFN-β + TNF-α (25 ng/mL + 10 ng/mL), for 4 hours. Scale bar – 200 μm, insert 30 μm (b) Expression of PYHIN family genes and *NLRP3* in undifferentiated human colonic organoids treated as in (a) and measured by RT-qPCR. (c) Expression of core inflammasome genes and regulated cytokine genes in undifferentiated colonic organoids treated as in (a) and measured by RT-qPCR. n=4 non-IBD organoid lines. Data are expressed as means ± SEM; 2-way ANOVA analysis was performed followed by Tukey's multiple comparisons test # p<0.05, ## p<0.01, ### p<0.001 versus untreated group, * p<0.05, ** p<0.01, *** p<0.001 as indicated.



Downloaded from journals.physiology.org/journal/ajpgi at Univ Col Cork (143.239.045.011) on October 3, 2022.

**Figure 7: Type I IFN treatment increases ZBP1-STING pathway gene expression in human colonic organoids**

(a) Expression of DNA sensors *ZBP1* and *cGAS* that induce type I IFNs measured by RT-qPCR in undifferentiated colonic organoids, treated with cytokines as per Figure 5. (b) Downstream pathway genes. (c) Type I IFN response biomarker genes. n=4 non-IBD organoid lines. Data are expressed as means ± SEM; 2-way ANOVA analysis was performed followed by Tukey's multiple comparisons test # $p<0.05$, ## $p<0.01$, ### $p<0.001$ versus control group, * $p<0.05$, ** $p<0.01$, *** $p<0.001$ as indicated.

**Figure 8: Co-treatment of human colonic organoids with type I or II IFN and TNF-α induces JAK dependent and inflammasome independent cell death and IL-1β/IL-18 secretion**

(a) Cell viability as determined by ATP content of differentiated and undifferentiated organoids treated as follows; 1) Ctrl (untreated), 2) BSA control (untreated), 3) IFN-γ - 10 ng/mL, 4) IFN-β - 10 ng/mL, 5) TNF-α - 10 ng/mL, 6) IFN-γ + TNF-α (10 ng/mL + 10 ng/mL) and 7) IFN-β + TNF-α (10 ng/mL + 10 ng/mL) for 24 hours. Data normalized to respective Ctrl (untreated) group for differentiated/undifferentiated organoids. n=2 independent biological experiments in duplicate, 2 non-IBD organoid lines (b) Released IL-1β and IL-18 detected in organoid supernatants by MSD, conditions as per (a), n=2 independent biological experiments in duplicate, 2 non-IBD organoid lines. (c) Cell viability as determined by ATP content of differentiated organoids treated with PBS/BSA, IFN-γ + TNF-α 10 ng/mL or IFN-β + TNF-α 10 ng/mL in combination with 1) Vehicle (0.2% DMSO, 0.1% $H_2O$), 2) JAK1/3 inhibitor Tofacitinib - 10 μM, 3) NLRP3 inhibitor MCC950 - 10 μM, 4) Caspase-1 inhibitor VX-765 - 50 μM, 5) Caspase-8 inhibitor Z-IETD-FMK - 50 μM, 6) VX-765 + Z-IETD-FMK (50 μM + 50 μM), and 7) Pan-Caspase inhibitor Z-VAD-FMK - 50 uM for 24 hrs. Data normalized to Ctrl (untreated) group. n=3 independent replicates in duplicate, non-IBD organoid line. (d) Released IL-1β and IL-18 detected in differentiated organoid supernatant by MSD, all conditions as per (c), each experimental replicate was normalized to the average pg/mL released from all samples within the experiment and expressed as fold change of average secretion (raw pg/mL values can be found in Figure S6d). n=3 independent replicates in duplicate for IL-1β and n=2 in duplicate for IL-18, non-IBD organoid line. (e) Live phase contrast and fluorescent microscopy (40x objective lens), consisting of transmission and GFP channel overlay, organoids treated as per (c) conditions 1 and 2, organoids incubated with SYTOX Green prior to imaging, representative images of n=2 independent experiments, non-IBD line. Scale bar - 50 μm. Data are expressed as means ± SEM; (a, b, c, d) two-way ANOVA analysis was performed followed by Bonferroni

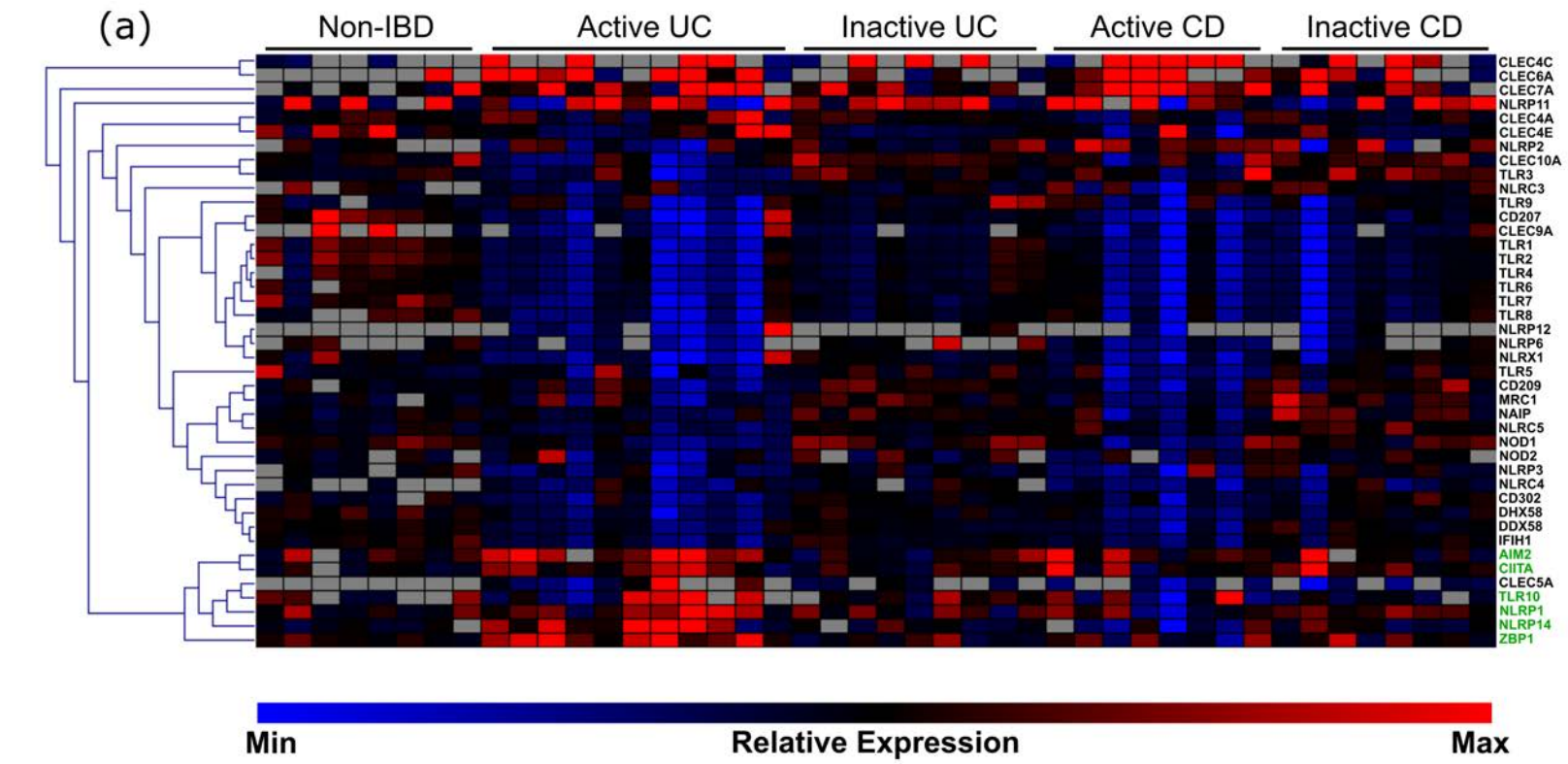


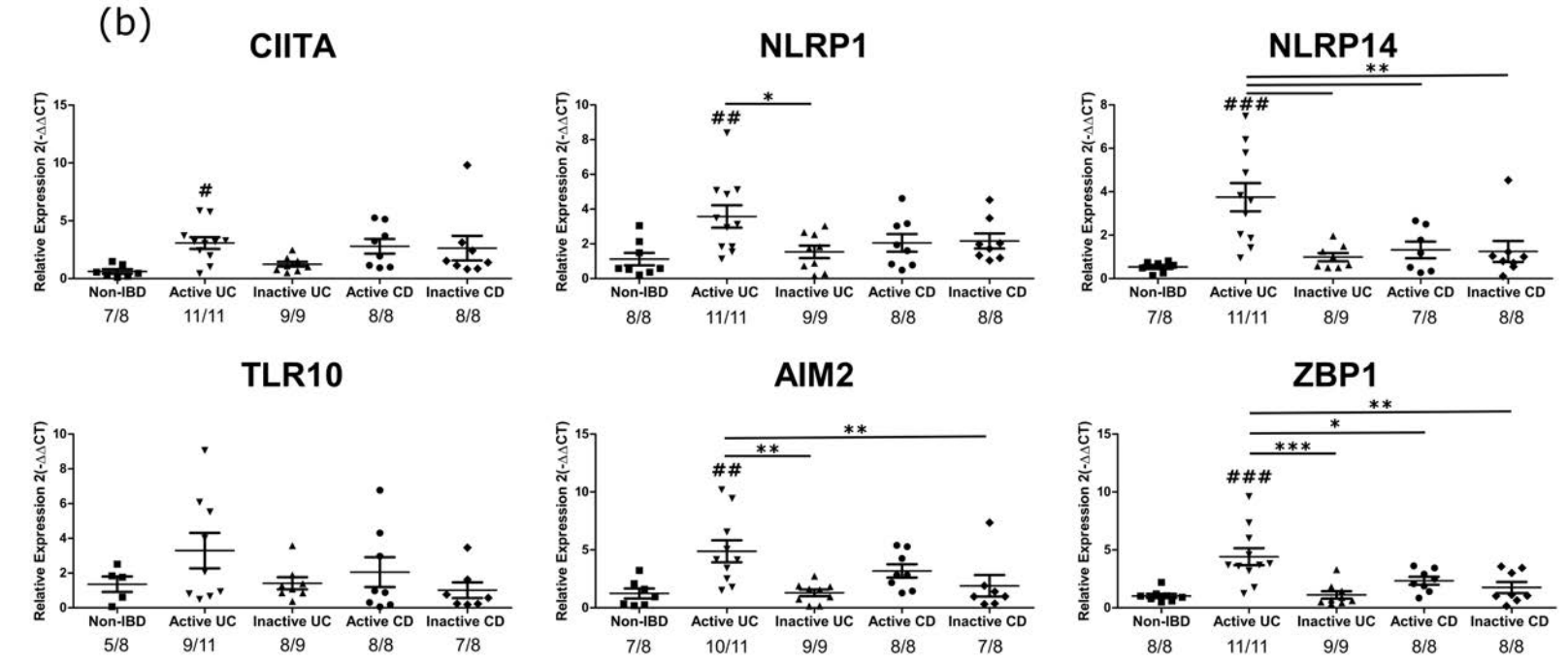
Downloaded from journals.physiology.org/journal/ajpgi at Univ Col Cork (143.239.045.011) on October 3, 2022.

1284 post-tests, versus undifferentiated Ctrl (# p<0.05, ## p<0.01, ### p<0.001) or differentiated
1285 Ctrl (~ p<0.05, ~~ p<0.01, ~~~ p<0.001), * p<0.05, ** p<0.01, *** p<0.001 as indicated.
1286
1287

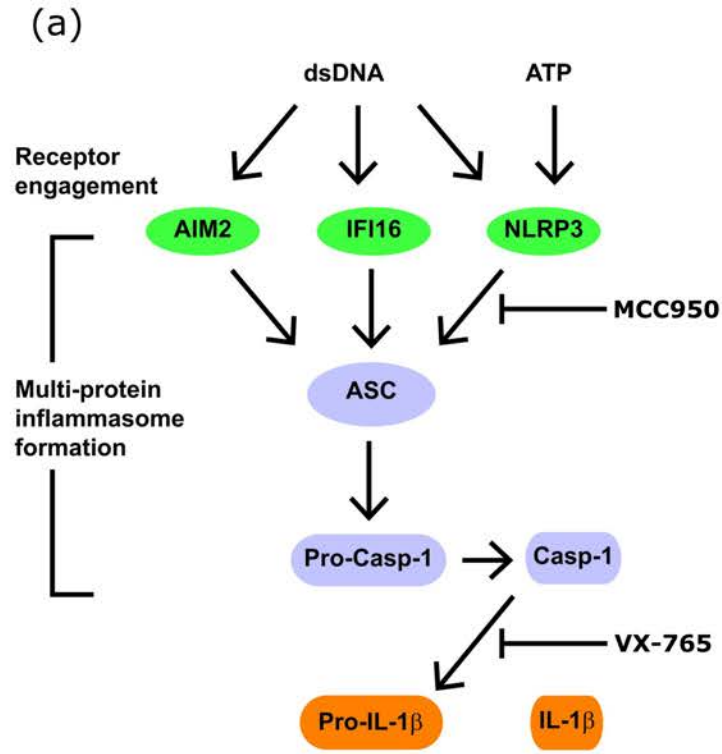


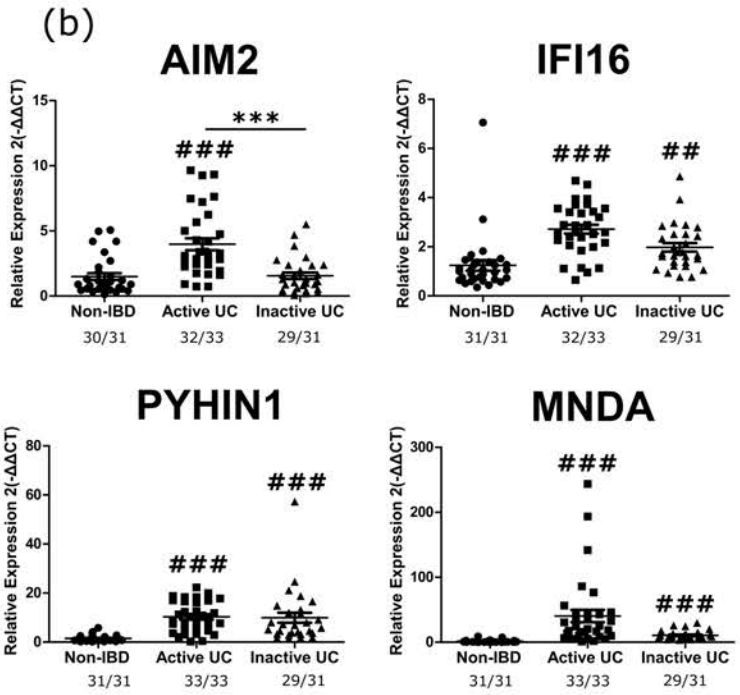
Downloaded from journals.physiology.org/journal/ajpgi at Univ Col Cork (143.239.045.011) on October 3, 2022.

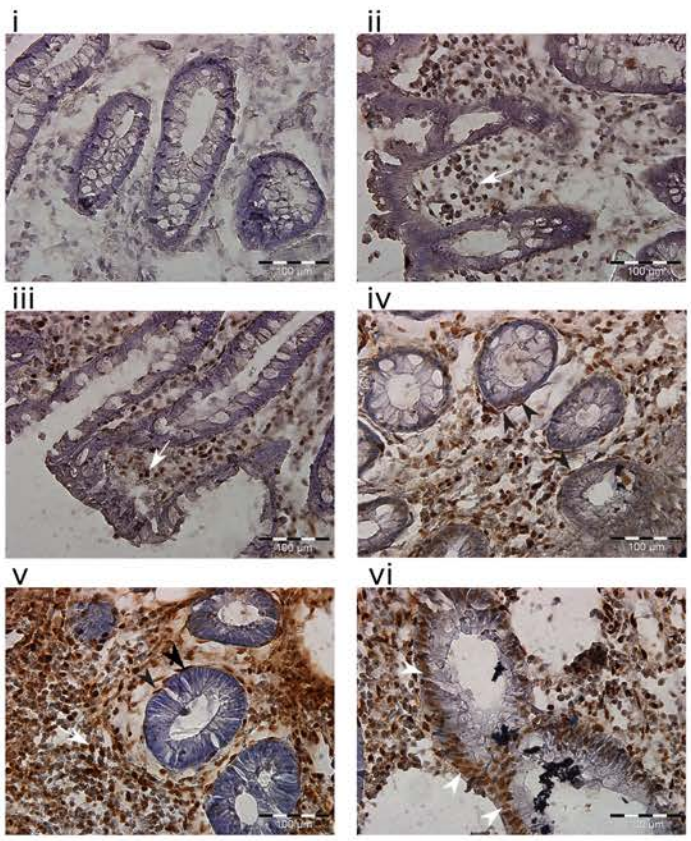


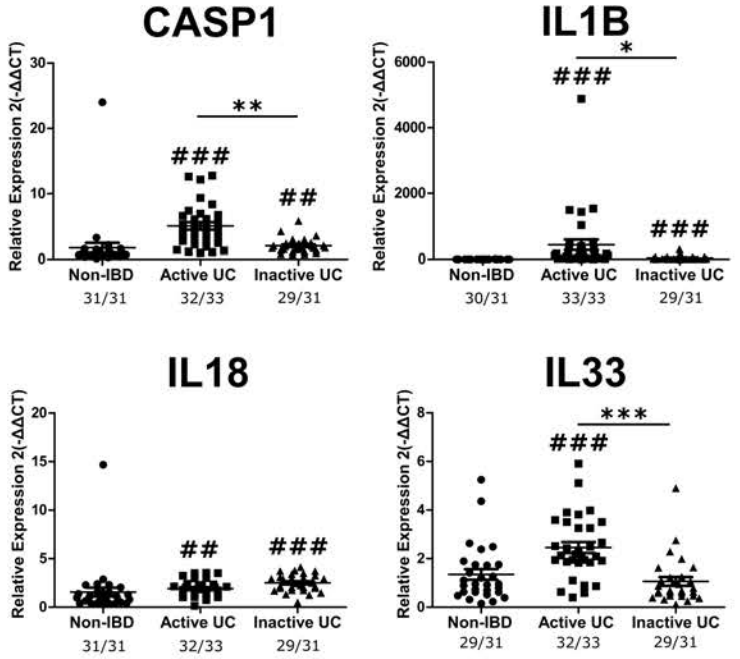



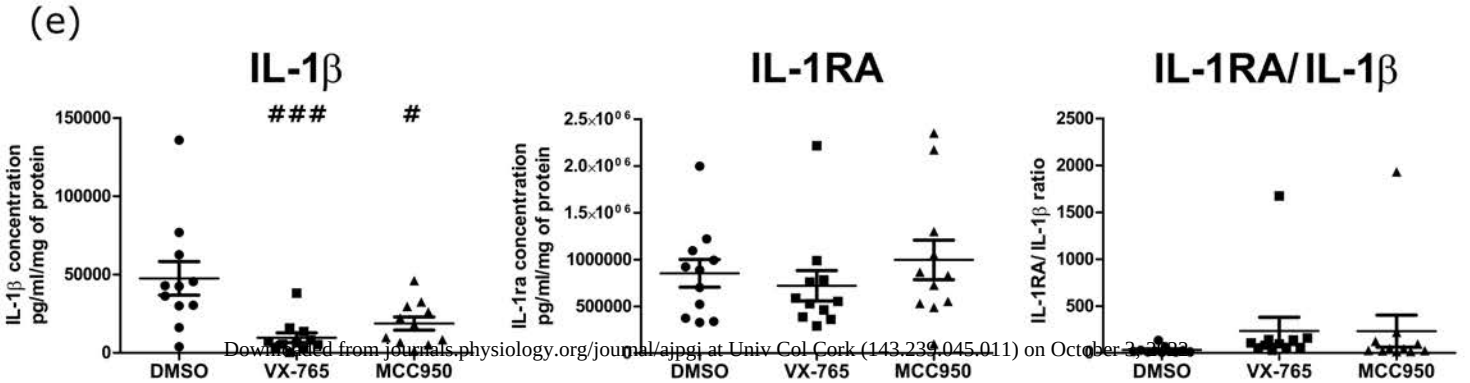

Downloaded from journals.physiology.org/journal/ajpgi at Univ Col Cork (143.239.045.011) on October 3, 2022.



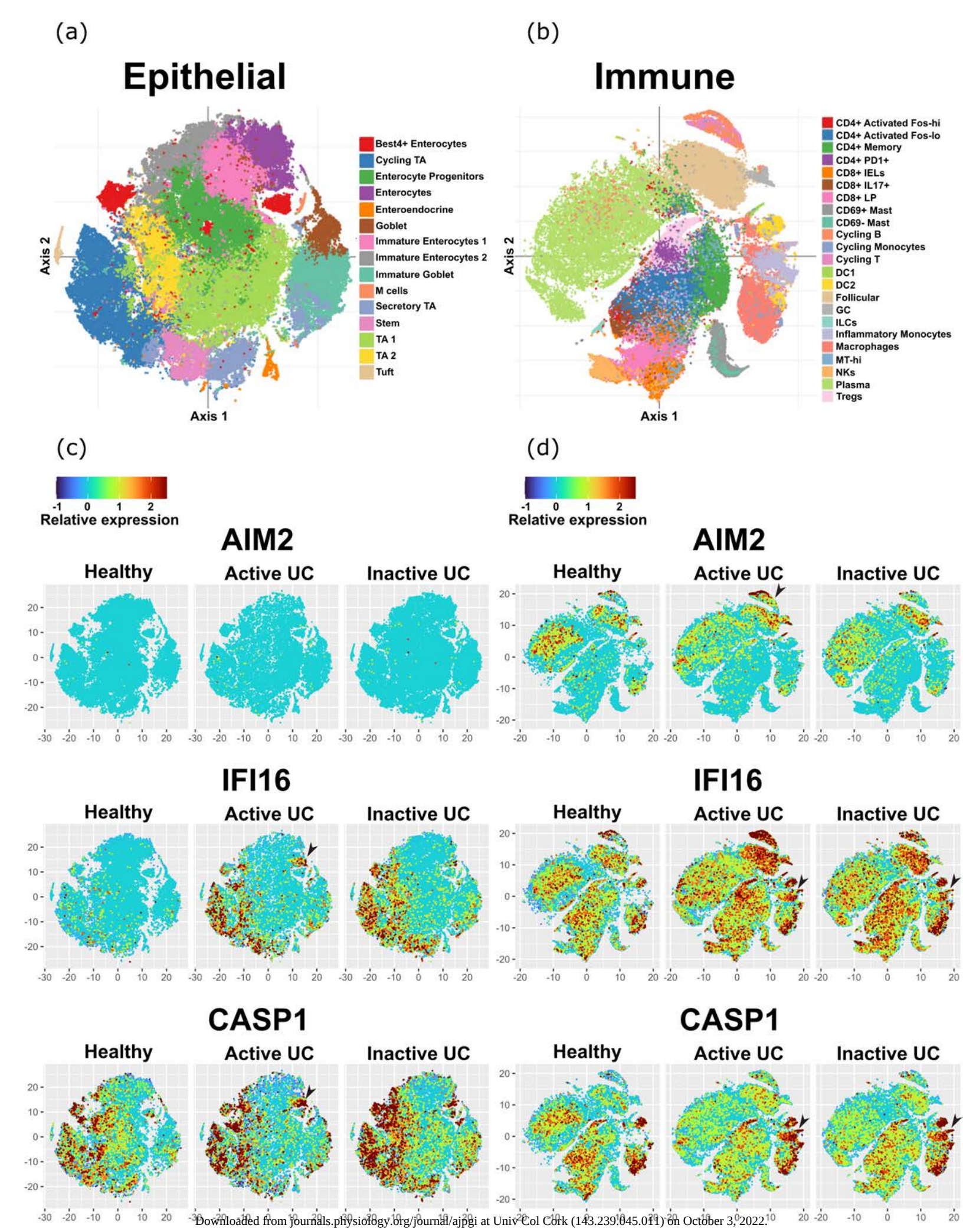



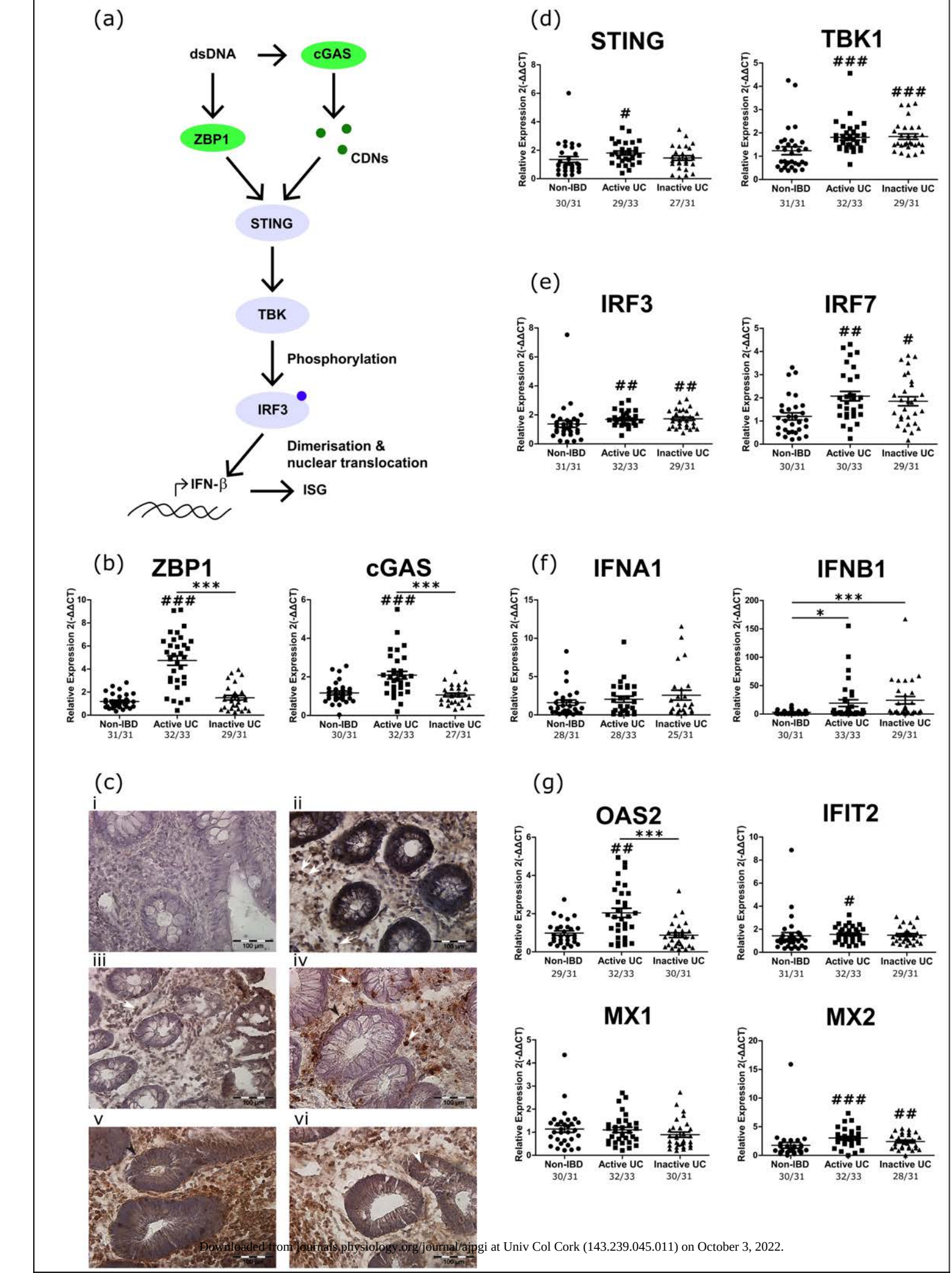



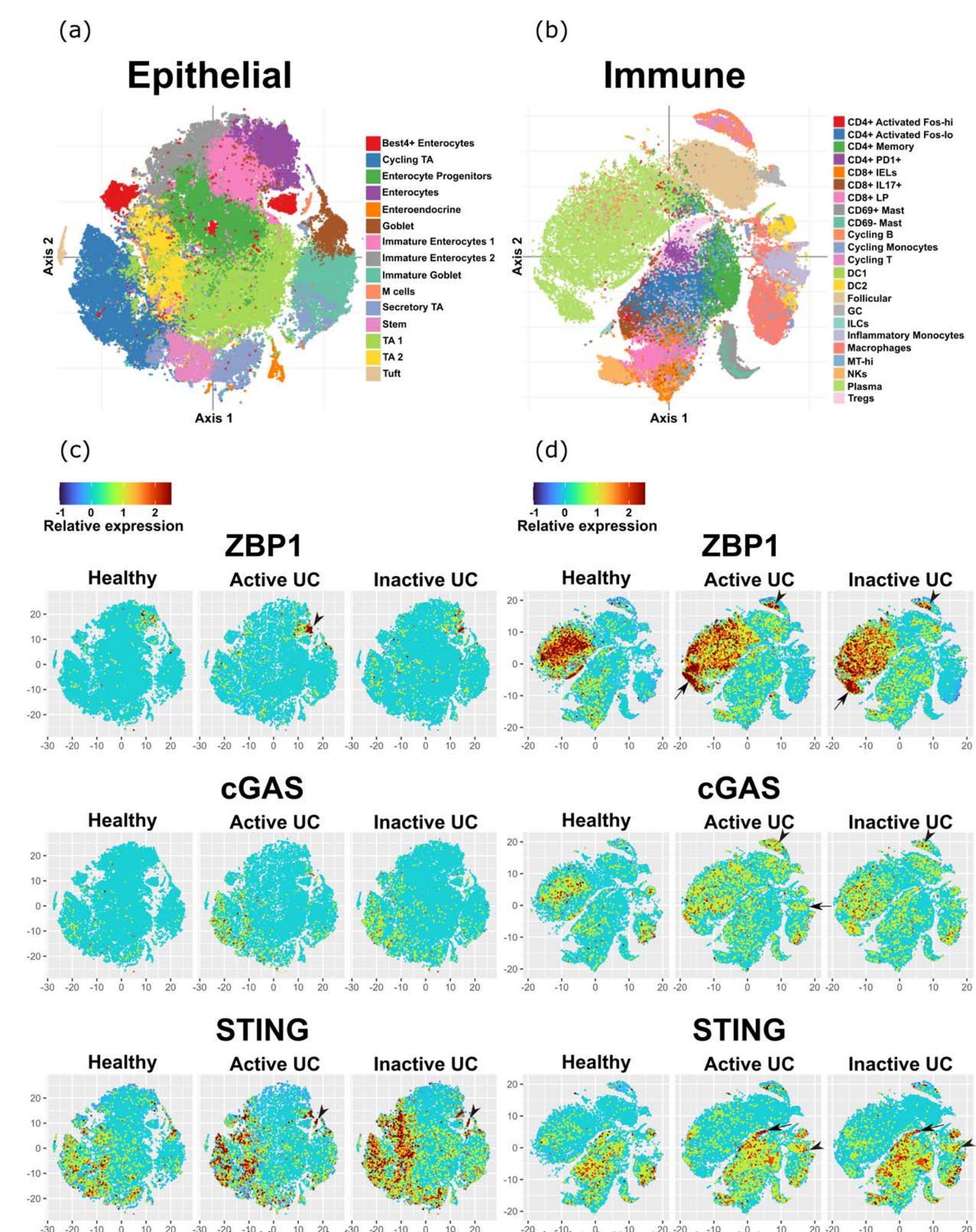

Downloaded from journals.physiology.org/journal/ajpgi at Univ Col Cork (143.239.045.011) on October 2x,2023.



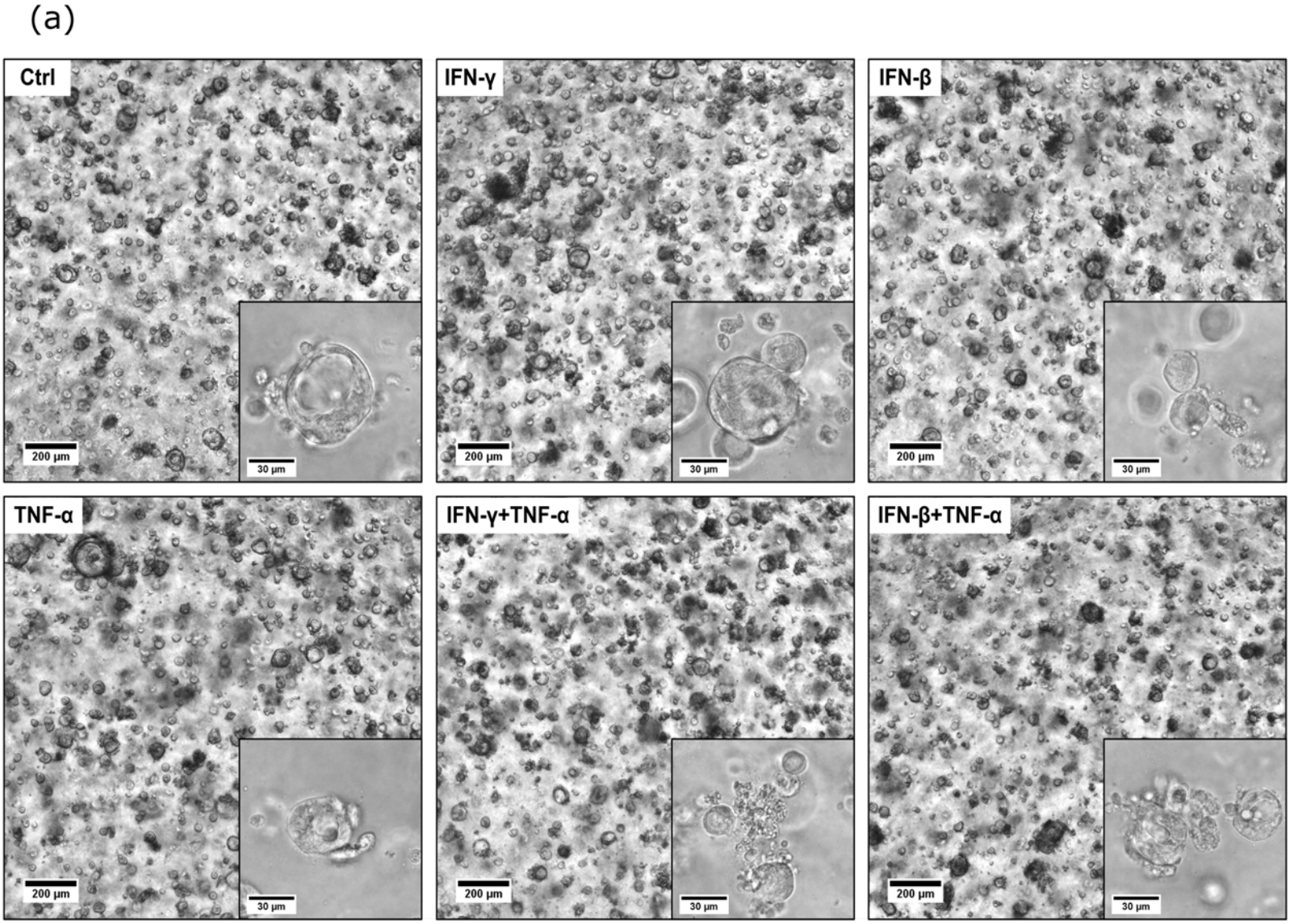

Downloaded from journals.physiology.org/journal/ajpgi at Univ Col Cork (143.239.045.011) on October 3, 2022.

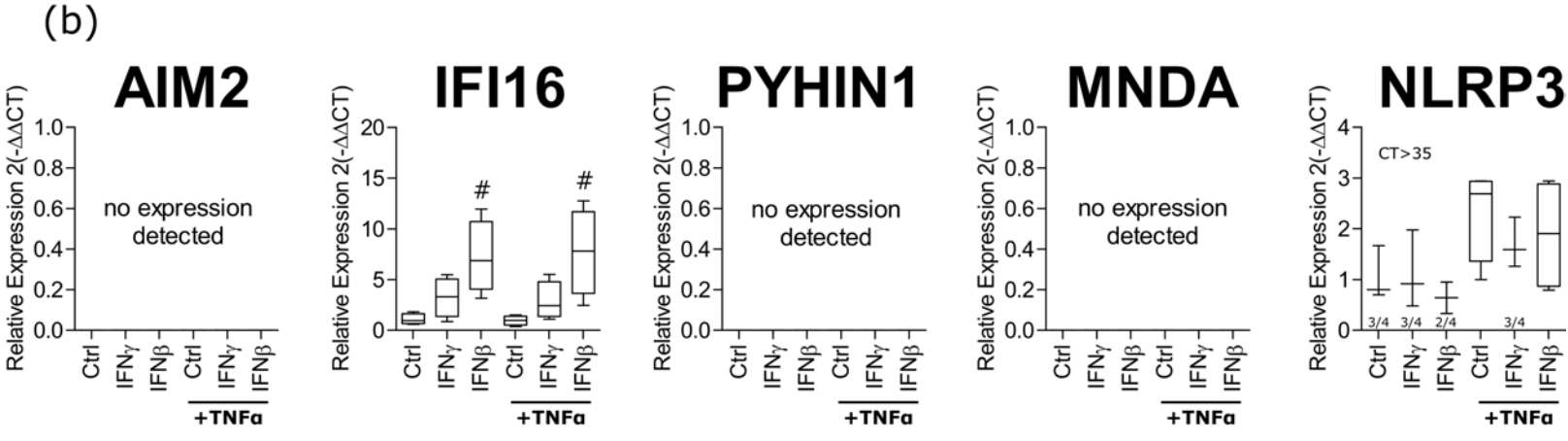


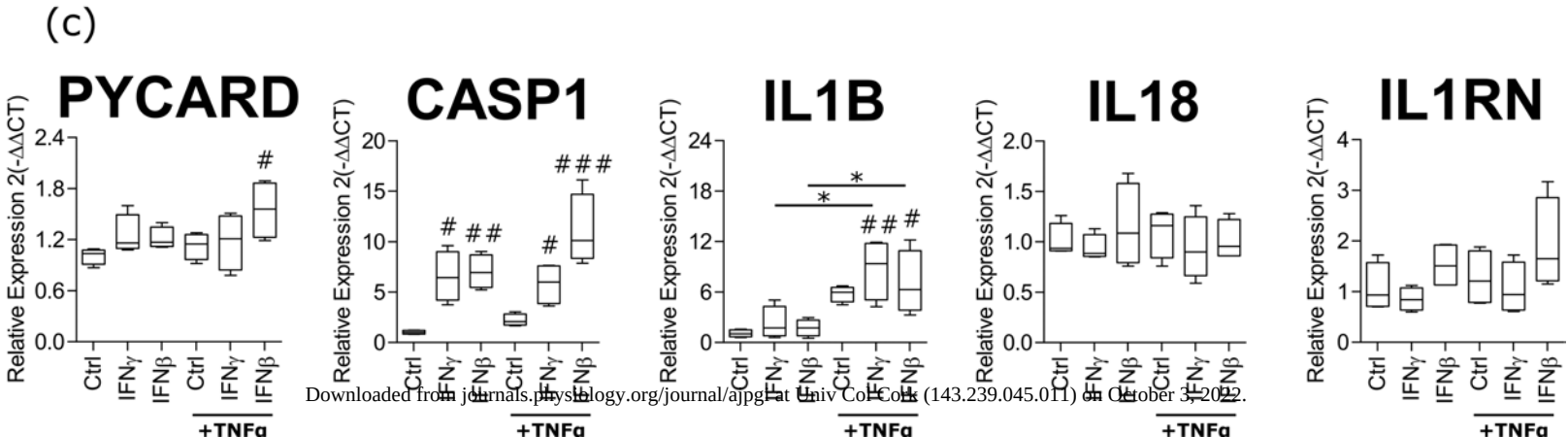

Downloaded from journals.physiology.org/journal/ajpgi at Univ Col Cork (143.239.045.011) on October 3, 2022.




Downloaded from journals.physiology.org/journal/ajpgi at Univ Col Cork (143.239.045.011) on October 3, 2022.

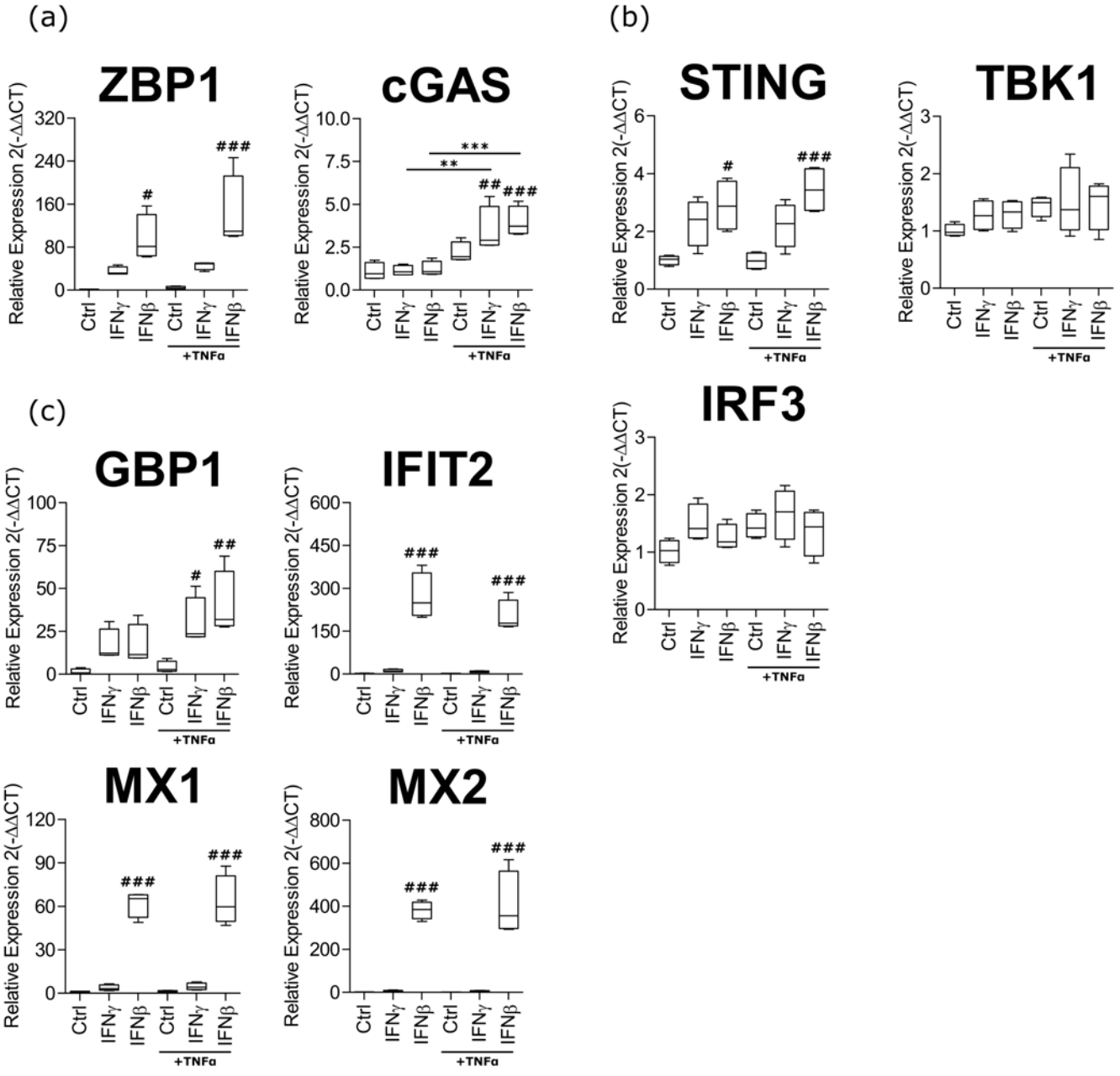


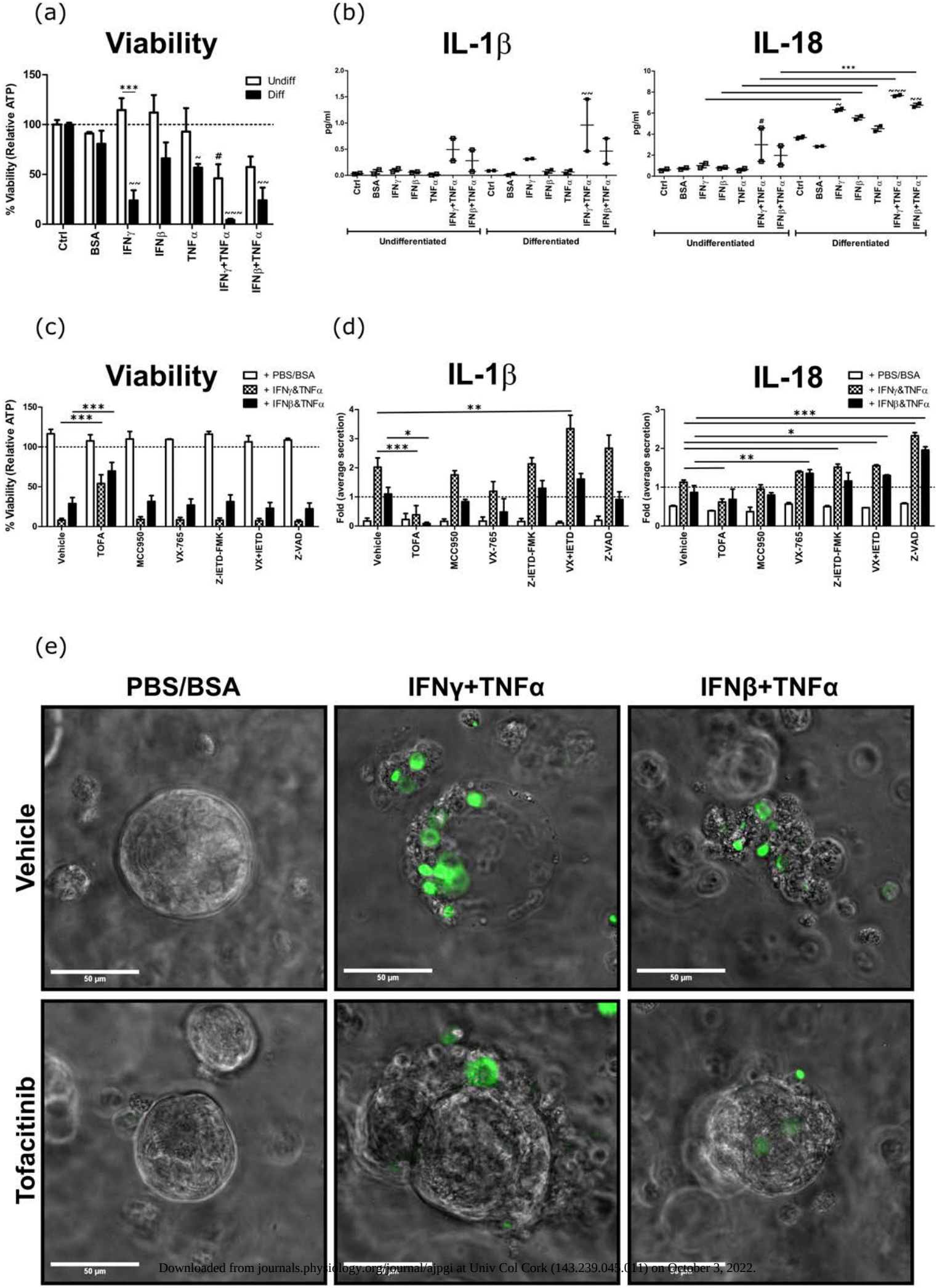




Downloaded from journals.physiology.org/journal/ajpgi at Univ Col Cork (143.239.045.011) on October 3, 2022.

# Figure 7




Downloaded from journals.physiology.org/journal/ajpgi at Univ Col Cork (143.239.045.011) on October 3, 2022.




Downloaded from journals.physiology.org/journal/ajpgi at Univ Col Cork (143.239.043.011) on October 3, 2022.

**Table 1.** Characteristics of IBD patients (cohort 1)

| | | Non-IBD (n = 8) | Active UC (n = 11) | Inactive UC (n = 9) | Active CD (n = 8) | Inactive CD (n = 8) |
|---|---|---|---|---|---|---|
| **Mean Age (years)** [a] | | 56.1 ± 13.6 | 44.7 ± 13.4 | 42.7 ± 14.5 | 36.1 ± 10.6 | 38.6 ± 11.4 |
| **Sex**[b] | **Male** | 5 (62.5%) | 7 (63.6%) | 4 (44.5%) | 1 (12.5%) | 3 (37.5%) |
| | **Female** | 3 (37.5%) | 4 (36.4%) | 5 (55.5%) | 7 (87.5%) | 5 (62.5%) |

[a]Age is represented as mean ± standard deviation. [b]Number of patients, followed by percentage of total in parentheses.

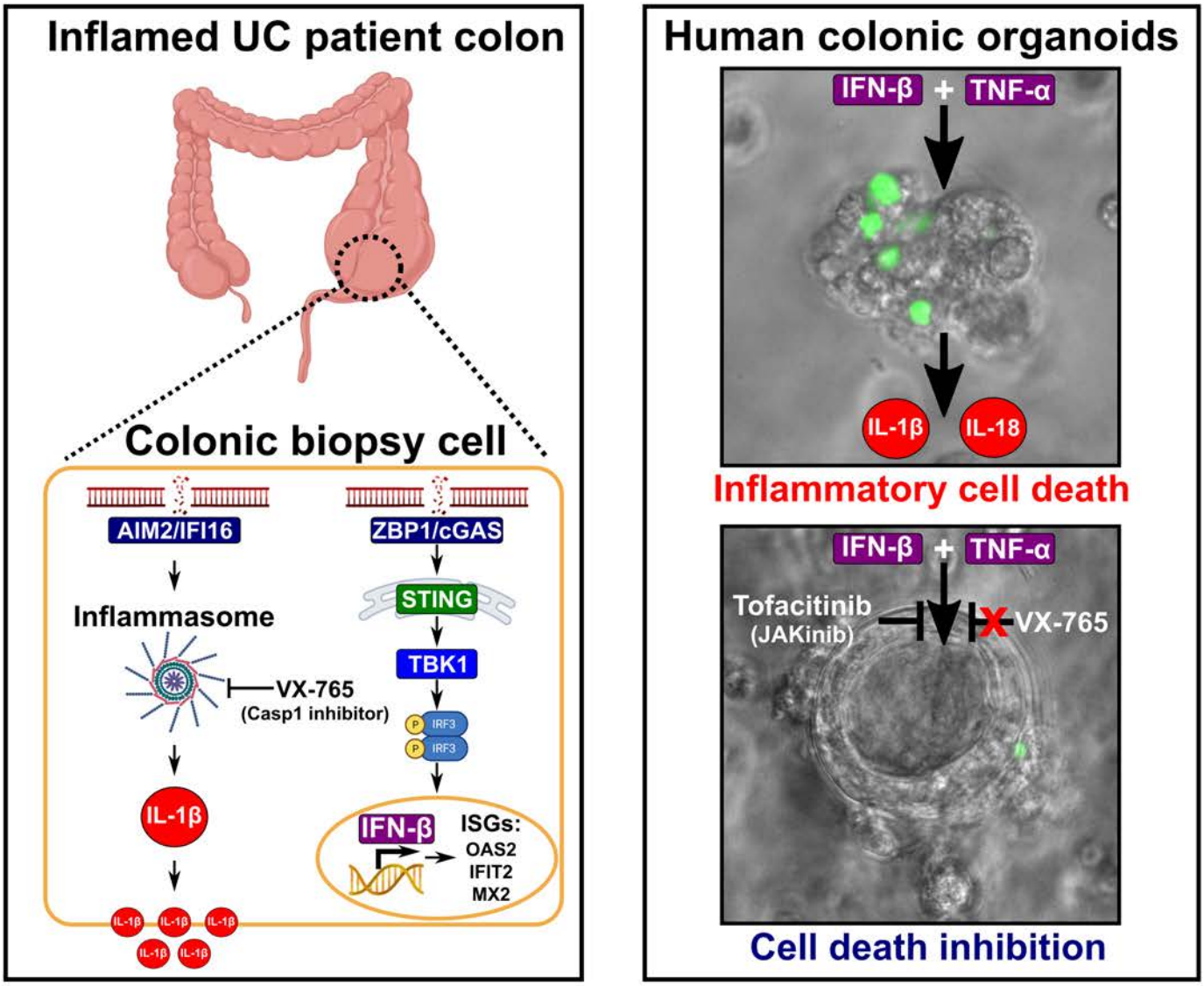
**Table 2.** Characteristics of UC patients (cohort 2)

| | | Non-IBD (n = 31) | Active UC (n = 33) | Inactive UC (n = 31) |
|---|---|---|---|---|
| **Mean Age (years)** [a] | | 53.6 ± 13.1 | 43.5 ± 13.9 | 48.7 ± 13.5 |
| **Sex**[b] | **Male** | 15 (48.4%) | 17 (51.5%) | 15 (48.4%) |
| | **Female** | 16 (51.6%) | 16 (48.5%) | 16 (51.6%) |
| **Medications**[b] | **Sulfasalazines** | N/A | 1 (3.03%) | 3 (9.68%) |
| | **Aminosalicylates** | N/A | 27 (81.82%) | 21 (67.74%) |
| | **6-MPs** | N/A | 4 (12.12%) | 3 (9.68%) |
| | **PPIs** | N/A | 2 (6.06%) | 5 (16.13%) |
| | **Steroids** | N/A | 16 (48.49%) | 5 (16.13%) |
| | **Antibiotics** | N/A | 2 (6.06%) | 0 (0%) |
| | **Anti-TNFs** | N/A | 0 (0%) | 0 (0%) |
| | **Other** | N/A | 16 (48.49%) | 19 (61.29%) |

Downloaded from journals.physiology.org/journal/ajpgi at Univ Col Cork (143.239.045.011) on October 3, 2022.

[a]Age is represented as mean ± standard deviation. [b]Number of patients, followed by percentage of total in parentheses.

Downloaded from journals.physiology.org/journal/ajpgi at Univ Col Cork (143.239.045.011) on October 3, 2022.




Downloaded from journals.physiology.org/journal/ajpgi at Univ Col Cork (143.239.045.011) on October 3, 2022.